Biogeochemistry (2021) 152:195–222
https://doi.org/10.1007/s10533-020-00748-6

# The fate of calcium in temperate forest soils: a Ca K-edge XANES study

**Jörg Prietzel · Wantana Klysubun · Luis Carlos Colocho Hurtarte**

Received: 3 April 2020 / Accepted: 12 December 2020 / Published online: 30 December 2020


**Abstract** Calcium (Ca) plays a crucial role for plant nutrition, soil aggregation, and soil organic matter (SOM) stabilization. Turnover and ecological functions of Ca in soils depend on soil Ca speciation. For the first time, we used synchrotron-based X-ray absorption near-edge structure (XANES) spectroscopy at the Ca K-edge (4038 eV) to investigate Ca speciation in soils. We present Ca K-edge XANES spectra of standard compounds with relevance in soils (e.g. calcite, dolomite, hydroxyapatite, anorthite, clay mineral-adsorbed Ca; Ca oxalate, formate, acetate, citrate, pectate, phytate). Calcium XANES spectra with good signal-to-noise ratios were acquired in fluorescence mode for Ca concentrations between 1 and 10 mg $g^{-1}$. Most standard spectra differed markedly among each other, allowing the identification of different Ca species in soils and other environmental samples as well as Ca speciation by linear combination fitting. Calcium XANES spectra obtained for samples from different horizons of twelve temperate forest soils revealed a change from dominating lithogenic Ca to clay mineral-bound and/or organically bound Ca with advancing pedogenesis. O layer Ca was almost exclusively organically bound. With increasing SOM decomposition, shares of oxalate-bound Ca decreased. Oxalate-bound Ca was absent in calcareous, but not in silicate subsoil horizons, which can be explained by microbial decomposition in the former vs. stabilization by association to pedogenic minerals in the latter soils. Synchrotron-based Ca XANES spectroscopy is a promising novel tool to investigate the fate of Ca during pedogenesis and—when performed with high spatial resolution (μ-XANES), to study aggregation and SOM stabilization mechanisms produced by Ca.

**Keywords** Ca speciation · Calcareous soils · Plant foliage · Silicate soils · Soil Ca forms · XANES spectroscopy

Responsible Editor: Edward Brzostek.

**Supplementary Information** The online version of this article (https://doi.org/10.1007/s10533-020-00748-6) contains supplementary material, which is available to authorized users.

J. Prietzel (✉) · L. C. C. Hurtarte
Chair of Soil Science, Center of Life and Food Sciences Weihenstephan, Technical University München, Emil-Ramann-Str. 2, 85354 Freising, Germany
e-mail: prietzel@wzw.tum.de

W. Klysubun
Synchrotron Light Research Institute, 111 Moo 6 University Avenue, Muang District, Nakhon Ratchasima 30000, Thailand

## Introduction

Calcium (Ca) in soils is an important nutrient element for plants and soil organisms (Marschner 1995;

Briedis et al. 2012; Paradelo et al. 2015). Soil contents of total Ca and/or exchangeable Ca are key factors of soil fertility. In addition, multivalent $Ca^{2+}$ cations play an important role for soil aggregation and structure formation by functioning as bridging cation (Wuddivira and Camps-Roach 2007; Clarholm and Skyllberg 2013; Rowley et al. 2018). This function is pivotal for soil carbon stabilization as either soil organic matter (SOM; Baldock and Skjemstad 2000; Grünewald et al. 2006; Mikutta et al. 2007; Whittinghill and Hobbie 2012; Clarholm and Skyllberg 2013; Rowley et al. 2018, 2020; Adhikari et al. 2019) or as soil secondary carbonates (Fernández-Ugalde et al. 2011; Rowley et al. 2018). After having entered the pedosphere via weathering of Ca-bearing minerals (carbonates, many silicates) and/or atmospheric deposition, Ca is cycled intensively through the soil–plant–microorganism system (Likens et al. 1998; Poszwa et al. 2000; Clarholm and Skyllberg 2013). It is taken up by plants via roots not only actively to meet their physiological demand, but also passively as part of the transpiration stream (Marschner 1995; Likens et al. 1998). Excess Ca is immobilized in plant foliage as Ca oxalate and other Ca carboxylates (e.g. polygalacturonate "pectate"), and recycled to the topsoil with the foliage litter (Marschner 1995; Likens et al. 1998; Franceschi and Nakata 2005; Clarholm and Skyllberg 2013). This mechanism decelerates or may even prevent topsoil acidification and base cation depletion ("base pumping effect", Poszwa et al. 2000; Clarholm and Skyllberg 2013). Whereas these processes generally are well known, little information exists about soil Ca speciation changes associated with Ca cycling through the soil–plant–microorganisms system.

In circumneutral and acidic soils, $Ca^{2+}$ cations can be directly bound to clay minerals (e.g. montmorillonite, smectite) and SOM. These compounds together store readily exchangeable, plant-available $Ca^{2+}$ in soils, which is a major contribution to soil base saturation (Clarholm and Skyllberg 2013). Moreover, $Ca^{2+}$ cations form stable complexes with SOM (Clarholm and Skyllberg 2013). These are mostly based on (i) outer-sphere sorption of $Ca^{2+}$ to deprotonated hydroxyl functional groups of phenolic compounds (Stevenson 1994; Grünewald et al. 2006; Kalinichev and Kirkpatrick 2007; Clarholm and Skyllberg 2013; Clarholm et al. 2015), (ii) chelate formation with deprotonated carboxyl groups (Stevenson 1994; Grünewald et al. 2006; Kalinichev and Kirkpatrick 2007), and (iii) formation of $Ca^{2+}$ bridges between negatively charged inorganic (e.g. clay minerals) and organic soil constituents (Kalinichev and Kirkpatrick 2007; Mikutta et al. 2007; Rowley et al. 2018). This interaction decreases microbial SOM decomposition (Castells and Penuelas 2003; Mikutta et al. 2007; Clarholm and Skyllberg 2013), and thus supports SOM accumulation (Rasmussen et al. 2018; Rowley et al. 2018, 2020).

During recent decades, synchrotron-based X-ray absorption spectroscopy, namely X-ray Absorption Near-Edge Structure (XANES) spectroscopy has emerged as a powerful technique for the speciation of many important elements in soils (Fendorf et al. 1994; Kelly et al. 2008). This technique enables a direct, non-invasive element speciation in soils and other materials based on species-specific X-ray attenuation patterns as a function of X-ray energy with respect to monochromatic X-rays irradiated on a sample of interest. Calcium K-edge XANES spectroscopy so far has been used in material science (Neuville et al. 2004; Proffit et al. 2016), biology (Sarret et al. 2007; Rajendran et al. 2013; Abe 2014; Thyrel et al. 2015), and in environmental science for investigating Ca mineral aerosols (Takahashi et al. 2008), coal chars (Liu et al. 2013), mine tailings (Blanchard et al. 2016), and—almost soil science—$CaCO_3$ granules excreted by earthworms (Brinza et al. 2014), but so far not for the investigation of soils; however, organic and inorganic Ca phosphate compounds in soils have been investigated by P K-edge XANES spectroscopy (e.g. Anderson et al. 2016; Prietzel et al. 2016a; Weyers et al. 2016). Here we demonstrate for the first time the applicability of synchrotron-based Ca XANES spectroscopy for direct, non-invasive quantification of different Ca forms in soils, and elucidation of Ca speciation changes during pedogenesis or Ca cycling in terrestrial ecosystems. In contrast to traditional techniques, the proposed method requires minimal (< 100 mg) sample amounts. It thus opens new perspectives for the quantification of different Ca species in soils and soil aggregates with small spatial resolution (< 1 cm), and for synchrotron-based Ca μ-XANES spectroscopy even with submicron resolution (Thyrel et al. 2015). In detail, we present Ca K-edge XANES spectra for different inorganic and organic Ca-bearing compounds with relevance in soils, and show that the spectra in most cases differ markedly among each

other. Moreover, we show that the Ca speciation of temperate forest soils differs among soil types and horizons. We relate the differences to ecosystem Ca cycling and transformation processes in the short term and pedogenesis in the long term.

## Material and methods

### Material

#### *Reference compounds*

We acquired Ca K-edge XANES spectra from fourteen inorganic and seven organic reference compounds with relevance as Ca-bearing soil constituents (Table 1). We studied different Ca carbonate minerals, Ca-bearing silicate and Ca sulfate minerals, as well as Ca halogenides and organic Ca-bearing compounds. We synthesized Ca phytate [hexacalcium (2,3,4,5,6-pentaphosphonatooxycyclohexyl) phosphate] and Ca pectate (Ca polygalacturonate), both important compounds for the function and structure of plants and microorganisms (Marschner 1995; de Kerchove and Elimelech 2007). For Ca phytate synthesis we treated inositol hexaphosphate, purchased from Sigma Aldrich Comp., with $Ca(OH)_2$ as described by Prietzel et al. (2016b), while for Ca pectate we treated polygalacturonic acid [$(C_6H_8O_6)_n$], purchased from Sigma Aldrich Comp., with saturated $Ca(OH)_2$ solution. The Ca polygalacturonate precipitate was neutralized with 0.01 M HCl to pH 5–6 to convert excess $Ca(OH)_2$ into $CaCl_2$, and removal of the $CaCl_2$ by repeated washing with deionized $H_2O$.

#### *Soil, geological parent material, and plant samples*

We also acquired Ca K-edge XANES spectra of samples from different horizons of various forest soils in Germany. We studied four initial soils developed on limestone or dolostone—Rendzic Leptosols according to the World Reference Base (IUSS Working Group WRB 2014)—at sites *Tuttlingen, Wellheim, Achenpass, Mangfall Mts.* (Table 2), and four soils with advanced pedogenesis (WRB: Eutric Cambisols) at the same sites. Additionally, we investigated two soils

**Table 1** Ca-bearing reference compounds used for K-edge XANES spectroscopy

| Compound mineral name | Ca form | Formula | Source |
|---|---|---|---|
| Calcite | Carbonate | $CaCO_3$, trigonal | Krantz Mineral Kontor |
| Aragonite | Carbonate | $CaCO_3$, orthorhombic | Krantz Mineral Kontor |
| Dolomite | Carbonate | $CaMgCO_3$ | Krantz Mineral Kontor |
| Apatite | Phosphate | $Ca_5(OH)(PO_4)_3$ | Sigma-Aldrich |
| Brushite | Phosphate | $CaHPO_4{\cdot}2H_2O$ | Sigma-Aldrich |
| Monetite | Phosphate | $CaHPO_4$ | Sigma-Aldrich |
| Anorthite | Silicate | $CaAl_2Si_2O_8$ | Krantz Mineral Kontor |
| Augite | Silicate | $Ca_2Si_2O_6$ | Krantz Mineral Kontor |
| Epidote | Silicate | $Ca_2Al_2(O\|OH\|SiO_4\|Si_2O_7)$ | Krantz Mineral Kontor |
| Ca adsorbed to montmorillonite | Silicate (adsorbed) | $Ca^{2+}$ adsorbed | Synthesized |
| Gypsum | Sulfate | $CaSO_4{\cdot}2H_2O$ | Krantz Mineral Kontor |
| Anhydrite | Sulfate | $CaSO_4$ | Sigma-Aldrich |
| Fluorite | Halogenide | $CaF_2$ | Sigma-Aldrich |
| Sinjarite | Halogenide | $CaCl_2$ | Sigma-Aldrich |
| Ca formate | Organic | $CaHCOO_2$ | Sigma-Aldrich |
| Ca acetate | Organic | $Ca(CH_3COO)_2$ | Sigma-Aldrich |
| Ca citrate | Organic | $C_{12}H_{10}Ca_3O_{14}$ | Sigma-Aldrich |
| Ca oxalate | Organic | $Ca_2C_2O_4$ | Sigma-Aldrich |
| Ca lactate | Organic | $C_6H_{10}CaO_6$ | Sigma-Aldrich |
| Ca pectate | Organic | $Ca_x(C_6H_8O_6)_y$ | Synthesized |
| Ca phytate | Organic + P | $C_6H_6Ca_6O_{24}P_6$ | Synthesized |

**Table 2** Important properties of the study sites

| *Site* soil types | Location | Parent material, profile exposition, inclination | Elevation [m a.s.l.] | Mean annual air temperature [°C] | Mean annual precipitation [mm] | Forest type |
|---|---|---|---|---|---|---|
| *Tuttlingen* Rendzic Leptosol, Eutric Cambisol | Swabian Alb (47° 59′ 16″ N 8° 44′ 47″ E) | Jurassic limestone Lept: NE slope, 25° Camb: Plateau | 750 | 6.5 | 850 | Mature *Fagus sylvatica* forest |
| *Wellheim* Rendzic Leptosol, Eutric Cambisol | Franconian Alb (48° 49′ 20″ N 11° 03′ 20″ E) | Jurassic limestone/dolostone Lept: Crest Camb: NW slope, 15° | Lept: 500 Camb: 460 | 7.7 | 780 | Mature *Fagus sylvatica* forest |
| *Achenpass* Rendzic Leptosol, Eutric Cambisol | German Alps (47° 35′ 43″ N 11° 37′ 54″ E) | Triassic dolostone NW slope, 30° | Lept: 1040 Camb: 1070 | 5.5 | 2110 | Mature mixed mountain forest *(Fagus sylvatica, Picea abies, Abies alba)* |
| *Mangfall Mts* Rendzic Leptosol Eutric Cambisol Folic Histosol | German Alps (47° 36′ 31″ N 11° 49′ 22″ E) | Triassic dolostone Lept: N slope, 30° Camb,Hist: S slope, 30° | 1060 | 6.8 | 1995 | Mature mixed mountain forest *(Fagus sylvatica, Picea abies, Abies alba)* |
| *Wetterstein* Folic Histosol | German Alps (47° 26′ 17″ N 11° 09′ 51″ E) | Triassic limestone Hist: N slope, 15° | 1450 | 3.5 | 1703 | Mature *Picea abies* mountain forest |
| *Bad Brückenau* Dystric Cambisol | Rhön Mts (50° 21′ 8″ N 9° 55′ 39″ E) | Basalt, crest | 810 | 6.0 | 960 | Mature *Fagus sylvatica* forest |
| *Steinach* Dystric Cambisol | Rhön Mts (50° 19′ 14″ N 10° 05′ 31″ E) | Basalt, S slope: 20° | 770 | 6.5 | 630 | Mature *Fagus sylvatica* forest |

*Lept* Rendzic Leptosol, *Camb* Eutric Cambisol, *Hist* Folic Histosol

with thick organic surface layers (WRB: Rockic Histosols; "Tangelrendzina" according to Kubiëna 1953) which had developed on limestone (*Wetterstein*) or dolostone (*Mangfall Mts.*), and two Dystric Cambisols (*Bad Brückenau, Steinach*) on basalt. Most soils have been described in detail earlier (e.g. Prietzel et al. 2013, 2016a); key parameters are presented in the Supporting Information (Table S1). For each profile, material was sampled by horizon from three different positions at the profile face which were pooled by horizon. In total, 64 unreplicated soil samples were included in our study. Bedrock was sampled from quarries or road cuttings in vicinity to the profiles. For each profile, we collected at least three bedrock pieces of a least 10 cm diameter. All bedrock pieces were crushed with a hammer, and unweathered interior

material from the crushed pieces was sampled and pooled. No bedrock sample was available for *Steinach*, however, we assume that the basalt parent material of *Steinach* has the same mineralogy as the basalt bedrock of the nearby (distance < 10 km) soil *Bad Brückenau*. We also acquired Ca K-edge XANES spectra of foliage sampled from important tree species at the study sites. Foliage samples included current-year and older needles of Norway spruce (*Picea abies*) and Silver fir (*Abies alba*) and leaves of European beech (*Fagus sylvatica*) and sycamore (*Acer pseudoplatanus*) from trees in the surrounding of the profiles. Foliage and fine roots in Ah horizons of the Leptosols and Cambisols were sampled at *Wellheim, Achenpass,* and *Mangfall Mts.* in autumn 2019.

## Methods

### *Sample pretreatment*

All soil samples were air-dried and sieved (2 mm mesh), and subsamples were fine ground for element analysis and Ca XANES spectroscopy. Additionally, all bedrock samples were finely ground. Foliage and root samples were dried at 40 °C for 1 week, cut into pieces, and then finely ground. Immediately after sampling, root samples were rinsed with water to remove attached soil particles.

### *Ca K-edge XANES spectroscopy*

In contrast to wet-chemical methods, synchrotron-based X-ray Absorption Near-Edge Structure (XANES) spectroscopy enables a direct, non-invasive Ca speciation in soils and other environmental samples. In that method, the sample under study is irradiated with energy-tuned monochromatic X-rays with high energy resolution in the energy range of either the K edge (Ca: 4038 eV), the L edges (Ca: 346 eV, 350 eV, 438 eV), or the M edges (Ca: 25 eV, 44 eV) of the element under study, and the attenuation of the X-ray signal as function of X-ray energy caused by the X-ray absorption of the sample is recorded. By comparison of the energy-dependent X-ray attenuation pattern of a sample with unknown Ca species composition with the energy-dependent X-ray attenuation patterns of reference compounds with known Ca speciation (i.e. spectrum deconvolution), the Ca speciation of the sample can be assessed. On ground subsamples of the reference compounds, soil, and plant samples, we acquired XANES spectra at the Ca K-edge at Beamline 8 of the Synchrotron Light Research Institute (SLRI) at Nakhon Ratchasima, Thailand (Klysubun et al. 2012, 2019). Briefly, we spread sample powder as a thin, homogeneous film on Ca-free Nitto tape (Nitto Denko Corp., Umeda, Japan) and mounted the tape on a sample holder. Samples with Ca concentrations > 20 mg $g^{-1}$ were diluted before analysis with finely ground ultra-pure quartz ($SiO_2$) powder to a concentration of 10 mg Ca $g^{-1}$ to avoid spectra distortion by self-absorption effects. Then we scanned the X-ray photon energy using an InSb(111) double-crystal monochromator with an energy resolution of $\Delta E/E = 3 \times 10^{-4}$. We recorded all spectra in fluorescence mode with a 13-element germanium detector. To increase fluorescence yield, we placed the sample holder at a 45° angle to the incident monochromatic beam (beam size 12 mm × 1 mm). We constantly purged the sample compartment with helium gas to minimize X-ray absorption by air surrounding the sample. We calibrated the monochromator with the second peak of pure $CaCO_3$ ($E_0$ = 4060.50 eV) according to Rajendran et al. (2013). This was repeated every 12 h, and no $E_0$ movement was noticed during the beamtime. After calibration, we acquired spectra in the energy range from 3940 to 4240 eV with a dwell time of one second per energy step. Energy steps were as follows: from 3940 to 4020 eV and from 4120 to 4240 eV: 5 eV; from 4020 to 4120 eV: 0.25 eV. For each sample, we acquired at least two spectra. Multiple spectra acquired for each sample always were identical, which rules out artificial sample changes caused by radiation damage. We merged replicate spectra obtained for a given sample using the software ATHENA (Ravel and Newville 2005). All merged spectra were subject to base-line correction (range 3980–4030 eV) and edge-step normalization (range 4120–4240 eV). The resulting spectra were deconvoluted by linear combination fitting (LCF) in the energy range 4020–4140 eV using up to five reference compounds. We identified the best fits by minimal R factors and good agreement between measured and modeled spectra in species-sensitive energy regions (signals reported in Table S3). Calcium species with > 5% contribution to total Ca as reported by LCF were assumed to be present in the respective sample.

**Table 3** Features of Ca K-edge XANES spectra of various standard compounds

| Compound | Ca form | Pre-edge 1 | Pre-edge 2 | Pre-edge 3 | White line | Post-edge 1 | Post-edge 2 | Post-edge 3 | Post-edge 4 | Post-edge 5 | Post-edge 6 | Post-edge 7 |
|---|---|---|---|---|---|---|---|---|---|---|---|---|
| Energy [eV] | | 4040/41 | 4045/46 | 4048/49 | **4050/51** | 4053/54 | 4056–58 | 4060–65 | 4066–72 | 4080–85 | 4089–90 | 4093–97 |
| Calcite | Carbonate | 4041 S | 4045 S | **4048.5 P** | 4050 P | | 4056 | **4060 P** | | 4081 P | | **4096** |
| Aragonite | Carbonate | 4041 P | 4046 S | 4049 P | **4050 P** | 4053 S | (4057) S | 4061 P | 4066 S | 4081.7 P | | 4092.7 P |
| Dolomite | Carbonate | 4041 S | 4045.5 S | **4048.3 P** | 4051.4 P | | 4058 S | **4062.5 P** | (4071.4) P | 4079.8 S | | **4096 P** |
| Apatite | Phosphate | 4040.4 P | 4045.7 S | | **4050.0 P** | | | 4061.5 S | (4071.5) P | 4080.5 P | | **4095 P** |
| Brushite | Phosphate | 4040.7 P | 4046 S | | **4050.8 P** | | 4056.8 S | 4064.7 S | (4071.8) P | **4080 S** | **4090–4095 P** | |
| Monetite | Phosphate | 4040.8 P | 4046 S | | **4051.0 P** | 4054 S | 4056.5 S | 4064.5 S | (4072.0) P | **4080 S** | **4090–4095 P** | |
| Epidote | Silicate | 4040.6 P | 4045.5 S | | **4049.7 P** | 4053.8 S | | (4063.6) P | (4072) P | 4080 P | | **4097 P** |
| Anorthite | Silicate | 4040.3 P | 4046 S | | **4050.7 P** | | 4058.1 P | 4063.8 S | (4071.4) P | 4081.1 S | | |
| Augite | Silicate | 4040.6 P | | 4047.8 S | **4050.8 P** | 4054.3 S | 4057.2 P | | | 4080 S | **4088.8 P** | |
| Ca montm | Silicate | 4040.7 P | 4046 S | | **4051 P** | | | 4062.9 S | (4072) P | 4080 S | | **4096 P** |
| Gypsum | Sulfate | 4040.5 P | 4045.8 S | 4049.3 S | **4051.2 P** | | | 4061.5 P | (4071.5) P | 4080.6 S | **4090 P** | |
| Anhydrite | Sulfate | 4040.7 P | 4046.3 S | | **4050.3 P** | 4054.1 S | | 4062.4 S | (4072) P | 4081.8 P | **4090 P** | |
| Fluorite | Halogenide | 4040.9 P | 4044.9 P | 4047.6 P | **4051.9 P** | | 4056.1 S | **4060.9 P** | 4069.4 S | **4081.5 P** | | **> 4095 P** |
| (Sinjarite) | Halogenide | 4040.7 P | 4045.8 S | 4047.8 S | **4048.8 P** | 4053 S | 4056S | 4064 P | (4071.5) P | 4081 S | | **4097 P** |
| Ca formate | Organic | 4040.5 S | | | **4050.4 P** | | | 4063.8 S | | **4080 S** | | **4097 P** |
| Ca acetate | Organic | 4040.5 S | 4043 S | | **4050.2 P** | | (4057) S | | (4071.4) P | **4080 P** | | **4096 P** |
| Ca citrate | Organic | 4040.5 P | 4043 S | | **4050.2 P** | | (4057.2) S | | (4071.4) P | **4080 S** | | |
| Ca oxalate | Organic | 4040.5 S | 4046 S | | **4050.5 P** | 4053.8 S | 4058 S | | (4071.4) P | 4080 S | **4090 P** | |
| Ca lactate | Organic | 4040.5 P | 4046 S | | **4050.5 P** | | | 4062.2 S | (4071.4) P | **4080 S** | | **4093 P** |
| Ca pectate | Organic | 4040.8 P | | | **4050.7 P** | | | 4055–4070 T | (4072.0) P | **4081 S** | | **4095 P** |
| Ca phytate | Organic + P | 4040.4 P | 4045.8 S | | **4050.9 P** | | | 4057–4070 T | (4071.8) P | **4080.5 S** | | **4095 P** |

*P* peak, *S* shoulder, *T* tailing

Bold type, underlined: key feature; bold type: prominent feature; in brackets: minor feature

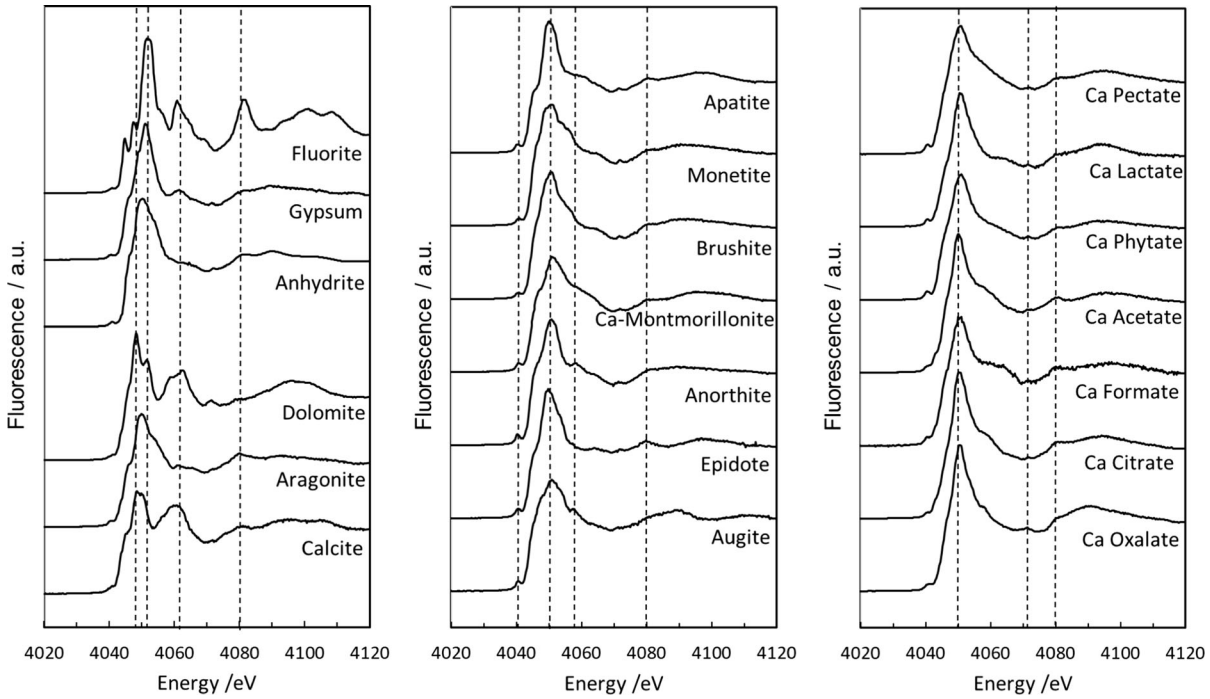


**Fig. 1** Baseline-corrected and normalized Ca K-edge XANES spectra of different reference compounds with potential relevance in soils. Left panel: Ca carbonates, sulfates, and fluorite. *Center panel* Ca silicates and phosphates. *Right panel* Organically bound Ca. All compounds were diluted to a Ca concentration of 10 mg $g^{-1}$

### *Determination of total element concentrations and general soil properties*

Concentrations of total C and N in all samples were determined by dry combustion at 1100 °C (EuroEA elemental analyzer, HEKAtech, Wegberg, Germany). We determined total concentrations of Ca, Mg, Fe, Al, and other cations in all samples by digestion with a mixture of hot concentrated $HF/HClO_4/HNO_3$ and analysis of the digests with ICP-OES (Varian Optima 3000). This method has been proven to result in complete element recovery in numerous earlier studies (e.g. Schwartz and Kölbel 1992; Hornburg and Lüer 1999; Prietzel et al. 2015). Good accuracy and precision of our C and N determination method has been proven by Prietzel and Christophel (2014). Furthermore, together with each sample batch a soil reference compound was analyzed as internal standard to assure good accuracy and precision of our total element analysis.

## Results

### Ca standard compounds

The baseline-corrected and edge-step normalized Ca K-edge XANES spectra of all reference standard compounds shared similar features (Table 3 and Fig. 1). For all standards except calcite and dolomite (white line peak at 4048.5 and 4048.3 eV, respectively), the largest peak (white line) was present at an energy of 4051 ± 1 eV. Additional pre-edge features were present at 4040/41 eV (shoulder for calcite, dolomite, and carboxylates; otherwise peaks), at 4045/46 eV (shoulders except for fluorite), and at 4048/49 eV (absent for carboxylate and phosphate compounds). Post-edge features were present at 4053/54 eV (shoulders), at 4057 ± 1 eV (mostly shoulders), and in the energy range 4060–4065 eV (peaks; shoulders, and tailings; particularly prominent for calcite, dolomite, and fluorite). Moreover, a small, but distinctive peak at 4071 eV, prominent post-edge features at 4080 eV, and peaks at 4089/4090 eV and

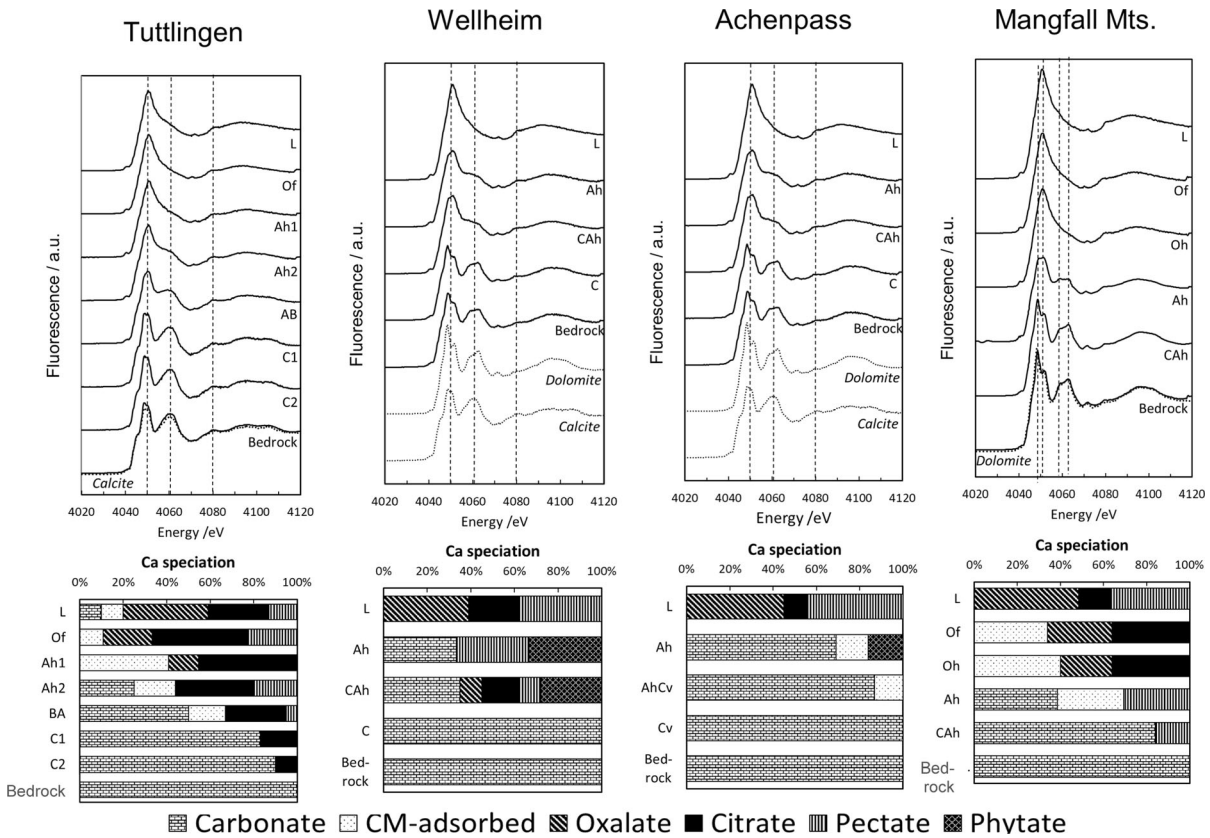


**Fig. 2** (Top panels) Normalized Ca K-edge XANES spectra and (bottom panels) contribution of different Ca species to total Ca in different horizons of Rendzic Leptosols formed from Limestone (*Tuttlingen*), dolomitic limestone (*Wellheim*) and dolostone (*Achenpass; Mangfall Mts.*) as determined by Linear combination fitting. Ca carboxylate species other than oxalate or pectate are summarized as Ca citrate. CM: Clay mineral

4093–4097 eV were present for almost all reference compounds.

Specific spectral features permit an unambiguous identification of different Ca carbonates (calcite, dolomite, aragonite), Ca sulfates (anhydrite, gypsum), and Ca fluorite, and discrimination of these compounds from Ca phosphates or Ca silicates on one hand as well as from organically bound Ca on the other (Fig. 1). The Ca silicate compounds augite, epidote, anorthite, and Ca adsorbed to montmorillonite also can be discriminated (Fig. 1; Figure S1). Particularly the spectrum of $Ca^{2+}$ adsorbed to a silicate mineral (montmorillonite) differs clearly from spectra of silicate minerals with structural Ca by its prominent shoulder at 4063 eV and the lack of a peak at 4057/58 eV (Figure S1). The spectra of the organic Ca compounds citrate, acetate, and lactate are similar and probably do not allow discrimination of these compounds. In contrast, the spectra of Ca oxalate, pectate, phytate, and formate differ markedly from one another as well as from the other organic Ca compounds (Figure S2). The differences are caused by a post-edge peak at 4090 eV (oxalate), tailings in the energy range 4055–4069 eV (pectate) or 4056–4070 eV (phytate), or a post-edge shoulder at 4064 eV (formate, lactate). The shapes of the Ca K-edge XANES spectra obtained in fluorescence mode for calcite that had been diluted with quartz to different concentrations from 1 up to 50 mg Ca $g^{-1}$ were identical. Spectra of calcite samples with larger Ca concentrations up to 50 mg $g^{-1}$ thus did not show any peak signal dampening due to self-absorption (Figure S3). For Ca oxalate, spectra obtained for the 20

and 50 mg Ca $g^{-1}$ variants showed moderate peak attenuation (Figure S3).

## Soils

### *Initial soils formed from calcareous parent material*

The parent material of the four Rendzic Leptosols differed concerning mineralogical composition and major Ca forms. The bedrock at *Tuttlingen* was limestone, and its Ca was calcite-bound, whereas the parent material of the other Leptosols was dolostone with dolomite-bound Ca. This was well reflected by the XANES results (Fig. 2). The Ca XANES spectra of all Leptosols changed systematically from subsoil to topsoil horizons, losing typical features of bedrock mineralogy. Carbonate-Ca signals were generally small in Ah horizons and absent in O layers. The decreased contribution of carbonate-Ca to total topsoil Ca was accompanied by an increased contribution of organically bound Ca (Fig. 2 and Table 4). Whereas the Ca in the C horizons of all Leptosols was exclusively or almost exclusively bound in calcite (*Tuttlingen*) or dolomite (other soils), Ah horizon Ca speciation differed markedly among the Leptosols. In the Ah of *Achenpass*, carbonate-bound Ca strongly dominated over clay mineral-adsorbed Ca and organically bound Ca. In the Ah of *Mangfall Mts.*, about equal Ca amounts were bound to carbonate, clay minerals, and SOM, and in the Ah horizons of *Wellheim* and *Tuttlingen,* organically bound Ca dominated. In the latter soil, inorganically bound Ca in the Ah horizon was carbonate-Ca, whereas in the former clay mineral-adsorbed Ca dominated. In the L layers of all Leptosols, oxalate-bound Ca was the dominating Ca species. With increasing soil depth, Ca oxalate concentrations and the contribution of oxalate-bound Ca to total Ca decreased systematically, and oxalate-bound Ca was absent in the mineral soil of all profiles except the carbonate-free Ah of *Tuttlingen*. Organically bound Ca in the Leptosol mineral soils was mostly present as Ca pectate or Ca phytate.

### *Soils with advanced pedogenesis formed from calcareous parent material*

Similar to the Leptosols, also the Ca XANES spectra of the samples taken from the four Cambisols at the calcareous study sites changed systematically from subsoil to topsoil horizons, losing or weakening the typical features of bedrock mineralogy. For *Tuttlingen* and *Wellheim,* no carbonate-Ca signals are visible in spectra of Bw and topsoil horizon samples, indicating the absence of carbonate-bound Ca (Fig. 3 and Table 5). For the alpine soils *Achenpass* and *Mangfall Mts.,* carbonate-Ca signals were also absent (*Mangfall Mts.*) or small (*Achenpass*) in the Bw horizons; however, the Ca XANES spectra of their Ah and O horizon samples showed distinct features of carbonate-bound Ca. Obviously, the topsoil horizons of the *Achenpass* and *Mangfall Mts.* Cambisols contain more carbonate-bound Ca than their Bw horizons. Furthermore, depth gradients of total Ca and carbonate C concentrations differed between the Cambisols *Tuttlingen* and *Wellheim* on one hand (increase with depth; Table S2) and the Cambisols *Achenpass* and *Mangfall Mts.* on the other (larger concentrations in Ah compared to B horizons). Results of XANES and traditional wet-chemical analysis thus both strongly indicate a minimum of carbonate-bound Ca in the B horizons of our alpine Cambisols formed from dolostone, whereas this was not the case for the non-alpine Cambisols formed from limestone. Concentrations of clay mineral-adsorbed Ca in Ah and Bw horizons of the Cambisols *Achenpass* and *Mangfall Mts.* were also larger than those in the respective horizons of the Cambisols *Tuttlingen* and *Wellheim*. As for the Leptosols, also in the Cambisols formed on calcareous bedrock, the contribution of organically bound Ca to total soil Ca decreased with soil depth. The Ca speciation of the Cambisol L layers was dominated by Ca pectate and Ca oxalate (Fig. 3) and thus similar to the L layer Ca speciation of the Leptosols. In contrast to the Leptosols, in all Cambisols except *Wellheim* the contribution of oxalate-bound Ca to organic Ca did not decrease with soil depth, and in many cases more than 30% of organically bound subsoil Ca was Ca oxalate.

### *Organic mountain soils formed on calcareous parent material (Rockic Histosols)*

As evident in the XANES spectra, carbonate-bound Ca was absent in the thick organic surface layers of both Histosols (Fig. 4) except for the Oh3 horizon of the *Mangfall Mts.* Histosol. Calcium concentrations increased moderately *(Wetterstein)* or markedly *(Mangfall Mts.)* with depth (Table 6), and the majority of soil Ca was organically bound. Inorganic Ca was

**Table 4** Ca speciation in initial soils (Rendzic Leptosols) formed from calcareous parent material as calculated by Linear Combination Fitting performed on Ca K-edge XANES spectra of the respective samples

| Horizon | Total Ca mg $g^{-1}$ | Carbonate Ca | Clay mineral sorbed Ca | Oxalate Ca | Citrate Ca | Pectate Ca | Phytate Ca | Organic Ca/ Total Ca | Organic $Ca_{exch}$/ Total $Ca_{exch}$ | Oxalate Ca/ Organic Ca | R factor LCF |
|---|---|---|---|---|---|---|---|---|---|---|---|
| *Rendzic Leptosol TUTTLINGEN* | | | | | | | | | | | |
| L | 21 | 2 | 2 | 8 | 6 | 3 | 0 | 0.80 | ND | 0.49 | 0.000405 |
| Of | 20 | 0 | 2 | 4 | 7 | 4 | 3 | 0.91 | 0.83 | 0.21 | 0.000588 |
| Ah1 | 11 | 0 | 3 | 1 | 3 | 0 | 4 | 0.73 | 0.65 | 0.12 | 0.000625 |
| Ah2 | 11 | 3 | 2 | 0 | 4 | 2 | 0 | 0.56 | 0.75 | 0 | 0.000574 |
| BwAh | 22 | 11 | 4 | 0 | 6 | 1 | 0 | 0.33 | 0.52 | 0 | 0.000348 |
| C1 | 53 | 44 | 0 | 0 | 9 | 0 | 0 | 0.17 | 1.0 | 0 | 0.001702 |
| C2 | 70 | 63 | 0 | 0 | 7 | 0 | 0 | 0.10 | 1.0 | 0 | 0.002444 |
| Bedrock | 362 | 362 | 0 | 0 | 0 | 0 | 0 | 0 | ND | – | |
| *Rendzic Leptosol WELLHEIM* | | | | | | | | | | | |
| L | 15 | 0 | 0 | 6 | 3 | 6 | 0 | 1.0 | ND | 0.39 | 0.010213 |
| Ah | 22 | 7 | 0 | 0 | 0 | 7 | 7 | 0.67 | ND | 0 | 0.000934 |
| CAh | 26 | 9 | 0 | 3 | 4 | 3 | 7 | 0.65 | ND | 0.15 | 0.000841 |
| C | 234 | 234 | 0 | 0 | 0 | 0 | 0 | 0 | 0 | – | 0.001265 |
| Bedrock | 233 | 234 | 0 | 0 | 0 | 0 | 0 | 0 | 0 | – | |
| *Rendzic Leptosol ACHENPASS* | | | | | | | | | | | |
| L | 16 | 0 | 0 | 7 | 2 | 7 | 0 | 1.0 | ND | 0.45 | 0.004626 |
| Ah | 105 | 72 | 16 | 0 | 0 | 0 | 17 | 0.16 | ND | 0 | 0.000321 |
| CAh | 103 | 90 | 13 | 0 | 0 | 0 | 0 | 0 | 0 | – | 0.000405 |
| C | 142 | 142 | 0 | 0 | 0 | 0 | 0 | 0 | 0 | – | |
| Bedrock | 215 | 215 | 0 | 0 | 0 | 0 | 0 | 0 | 0 | – | |
| *Rendzic Leptosol MANGFALL MTS* | | | | | | | | | | | |
| L | 16 | 0 | 0 | 8 | 2 | 6 | 0 | 1.0 | ND | 0.49 | 0.006533 |
| Of | 15 | 0 | 5 | 5 | 5 | 0 | 0 | 0.66 | 0.64 | 0.45 | 0.001648 |
| Oh | 41 | 0 | 16 | 10 | 15 | 0 | 0 | 0.60 | 0 | 0.40 | 0.002969 |
| Ah | 119 | 46 | 37 | 0 | 0 | 37 | 0 | 0.31 | 0 | 0 | 0.002163 |
| CAh | 177 | 149 | 0 | 0 | 0 | 28 | 0 | 0.16 | 0 | 0 | 0.001983 |
| Bedrock | 222 | 222 | 0 | 0 | 0 | 0 | 0 | 0.00 | 0 | – | |

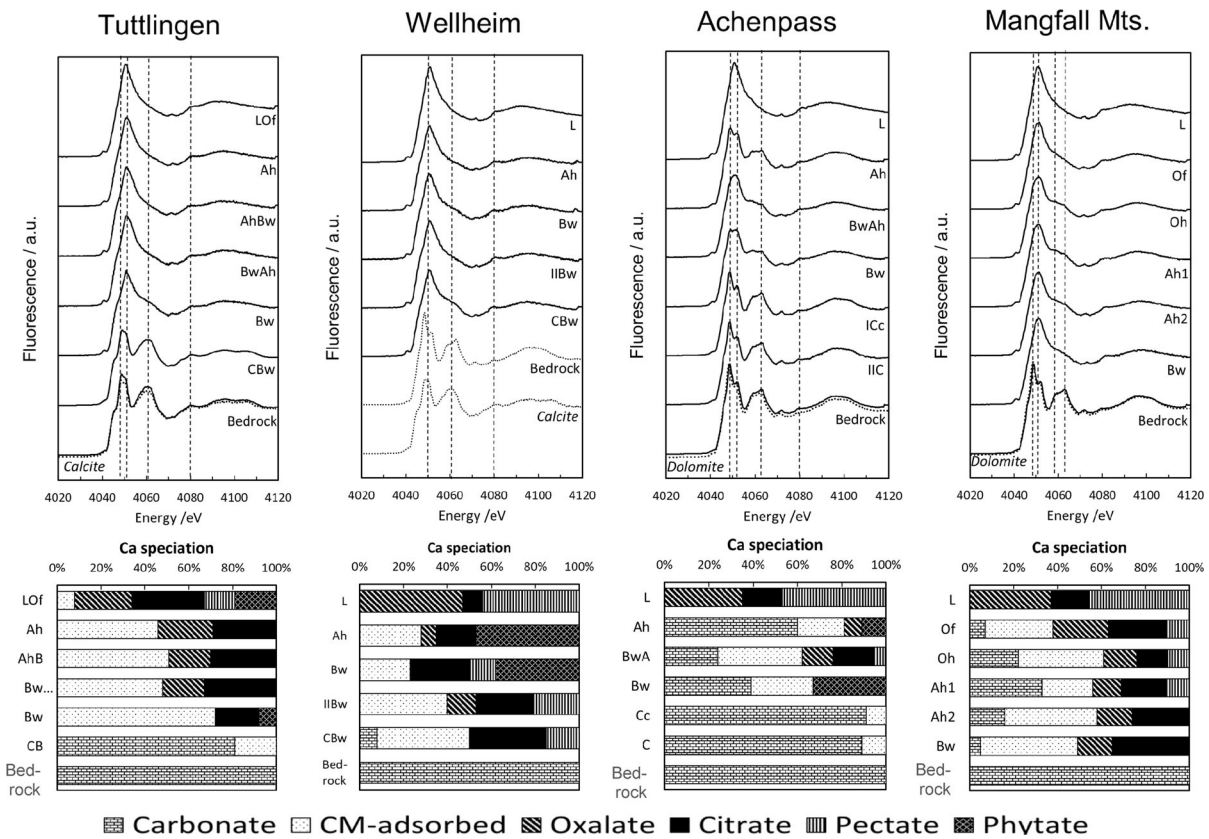


**Fig. 3** (Top panels) Normalized Ca K-edge XANES spectra and (bottom panels) contribution of different Ca species to total Ca in different horizons of Cambisols formed from Limestone (*Tuttlingen*), dolomitic limestone (*Wellheim*) and dolostone (*Achenpass; Mangfall Mts.*) as determined by Linear combination fitting. Ca carboxylate species other than oxalate or pectate are summarized as Ca citrate. CM: Clay mineral

clay-mineral bound (*Mangfall Mts.* Oh3: equal contribution of clay mineral-bound Ca and carbonate Ca). Among the organic Ca forms, the contribution of oxalate-bound Ca decreased with soil depth, SOM age, and SOM decomposition status. Oxalate-bound Ca dominated in the Of horizons of both Histosols, whereas non-oxalate organic Ca dominated in the Oh horizons. Ca pectate was enriched in lower, more decomposed Oh horizons.

### *Soils with intermediate pedogenesis formed from silicate parent material*

Calcium in the basalt parent material of the Dystric Cambisol *Bad Brückenau* was mainly bound in augite and plagioclase, the latter represented by our anorthite standard (Fig. 5). As reported before for the calcareous soils, also for the Cambisols with silicate parent material, XANES spectra changed systematically from subsoil to topsoil horizons. However, in contrast to the calcareous soils typical spectral features of bedrock minerals (e.g. the peak at 4057/58 eV, characteristic for plagioclase and augite) were present in the entire mineral soil of the basalt-derived Cambisols. This indicates the presence of bedrock minerals and predominance of primary silicate-bound Ca to total Ca in the fine earth fraction of the entire mineral soil (Fig. 5). In both Dystric Cambisols, clay mineral-adsorbed Ca was enriched in the O layer, but most Ca was organically bound. In the mineral soil of *Steinach*, the contribution of organically bound Ca to total Ca decreased systematically with depth. For the *Bad Brückenau* Cambisol, the contribution of organically bound Ca to total soil Ca generally was larger

**Table 5** Ca speciation in soils with advanced pedogenesis (Eutric Cambisols) formed from calcareous parent material as calculated by Linear Combination Fitting performed on Ca K-edge XANES spectra of the respective samples. Bedrock Ca speciation of different sites: see Table 4

| Horizon | Total Ca | Carbonate Ca | Clay mineral sorbed Ca | Oxalate Ca | Citrate Ca | Pectate Ca | Phytate Ca | Organic Ca/Total Ca | Organic $Ca_{exch}$/ Total $Ca_{exch}$ | Oxalate Ca/ Organic Ca | R factor LCF |
|---|---|---|---|---|---|---|---|---|---|---|---|
| | mg $g^{-1}$ | | | | | | | | | | |
| *Eutric Cambisol TUTTLINGEN* | | | | | | | | | | | |
| LOf | 9 | 0 | < 1 | 2 | 3 | 1 | 2 | 0.92 | 0.92 | 0.28 | 0.000546 |
| Ah | 5 | 0 | 2 | 1 | 2 | 0 | 0 | 0.54 | 0.41 | 0.46 | 0.001987 |
| AhBw | 3 | 0 | 2 | < 1 | 1 | 0 | 0 | 0.49 | 0.44 | 0.39 | 0.001966 |
| BwAh | 4 | 0 | 2 | < 1 | 1 | 0 | 0 | 0.52 | 0.51 | 0.37 | 0.002785 |
| Bw | 7 | 0 | 5 | 0 | 1 | 0 | < 1 | 0.28 | 0.13 | 0 | 0.000621 |
| CB | 135 | 109 | 26 | 0 | 0 | 0 | 0 | 0 | 0 | – | 0.002485 |
| *Eutric Cambisol WELLHEIM* | | | | | | | | | | | |
| L | 18 | 0 | 0 | 9 | 2 | 8 | 0 | 1.0 | ND | 0.47 | 0.003939 |
| Ah | 2 | 0 | < 1 | < 1 | < 1 | 0 | 1 | 0.72 | 0.44 | 0.10 | 0.000786 |
| Bw | 2 | 0 | < 1 | 0 | < 1 | < 1 | < 1 | 0.77 | 0.54 | 0 | 0.000883 |
| II Bw | 4 | 0 | 1 | < 1 | < 1 | < 1 | 0 | 0.60 | 0.44 | 0.22 | 0.001249 |
| CBw | 9 | < 1 | 0 | 0 | 6 | 1 | 0 | 0.50 | ND | 0 | 0.000626 |
| *Eutric Cambisol ACHENPASS* | | | | | | | | | | | |
| L | 16 | 0 | 0 | 6 | 3 | 8 | 0 | 1.0 | ND | 0.35 | 0.004465 |
| Ah | 38 | 23 | 8 | 3 | 0 | 0 | 4 | 0.19 | ND | 0.42 | 0.000595 |
| BwAh | 17 | 4 | 7 | 2 | 3 | 1 | 0 | 0.38 | ND | 0.37 | 0.000526 |
| Bw | 13 | 5 | 4 | 0 | 0 | 0 | 4 | 0.33 | ND | 0 | 0.000430 |
| BwC | 158 | 144 | 14 | 0 | 0 | 0 | 0 | 0 | 0 | – | 0.001672 |
| (Bw)C | 170 | 151 | 19 | 0 | 0 | 0 | 0 | 0 | 0 | – | 0.003565 |
| *Eutric Cambisol MANGFALL MTS* | | | | | | | | | | | |
| L | 17 | 0 | 0 | 6 | 3 | 8 | 0 | 1.0 | ND | 0.37 | 0.002513 |
| Of | 20 | 1 | 6 | 5 | 5 | 2 | 0 | 0.62 | 0.48 | 0.40 | 0.001293 |
| Oh | 24 | 5 | 9 | 4 | 3 | 2 | 0 | 0.39 | 0.33 | 0.38 | 0.000689 |
| Ah1 | 29 | 10 | 7 | 4 | 6 | 3 | 0 | 0.44 | 0.56 | 0.30 | 0.000602 |
| Ah2 | 24 | 4 | 10 | 4 | 6 | 0 | 0 | 0.42 | 0.22 | 0.38 | 0.000793 |
| Bw | 15 | < 1 | 7 | 2 | 5 | 0 | 0 | 0.51 | 0.27 | 0.31 | 0.001273 |

than at *Steinach* and showed no depth trend. Most organically bound Ca was oxalate-bound (Table 6).

Plant samples

Tree foliage Ca concentrations (Table 7) decreased in the order sycamore > beech > fir > spruce. Foliage Ca speciation differed (Fig. 6) between broadleaf (50% oxalate-bound Ca; 40% pectate Ca; 10% phytate Ca) and conifer species (90% oxalate-bound Ca; 10% citrate-Ca). No Ca speciation difference was present between current-year and older conifer needles. Fine root Ca concentrations were two to four times larger for beech on Leptosols or Cambisols with calcareous bedrock compared to spruce stocking on the Folic Histosol (Table 7). Beech fine root Ca speciation was almost identical among sites. It differed markedly from that of beech foliage by larger shares of Ca pectate (55% of total Ca) and Ca phytate (25%), and smaller oxalate-bound Ca shares (20%). Spruce root Ca was 33% oxalate, 33% pectate, 26% citrate, and 9% phytate.

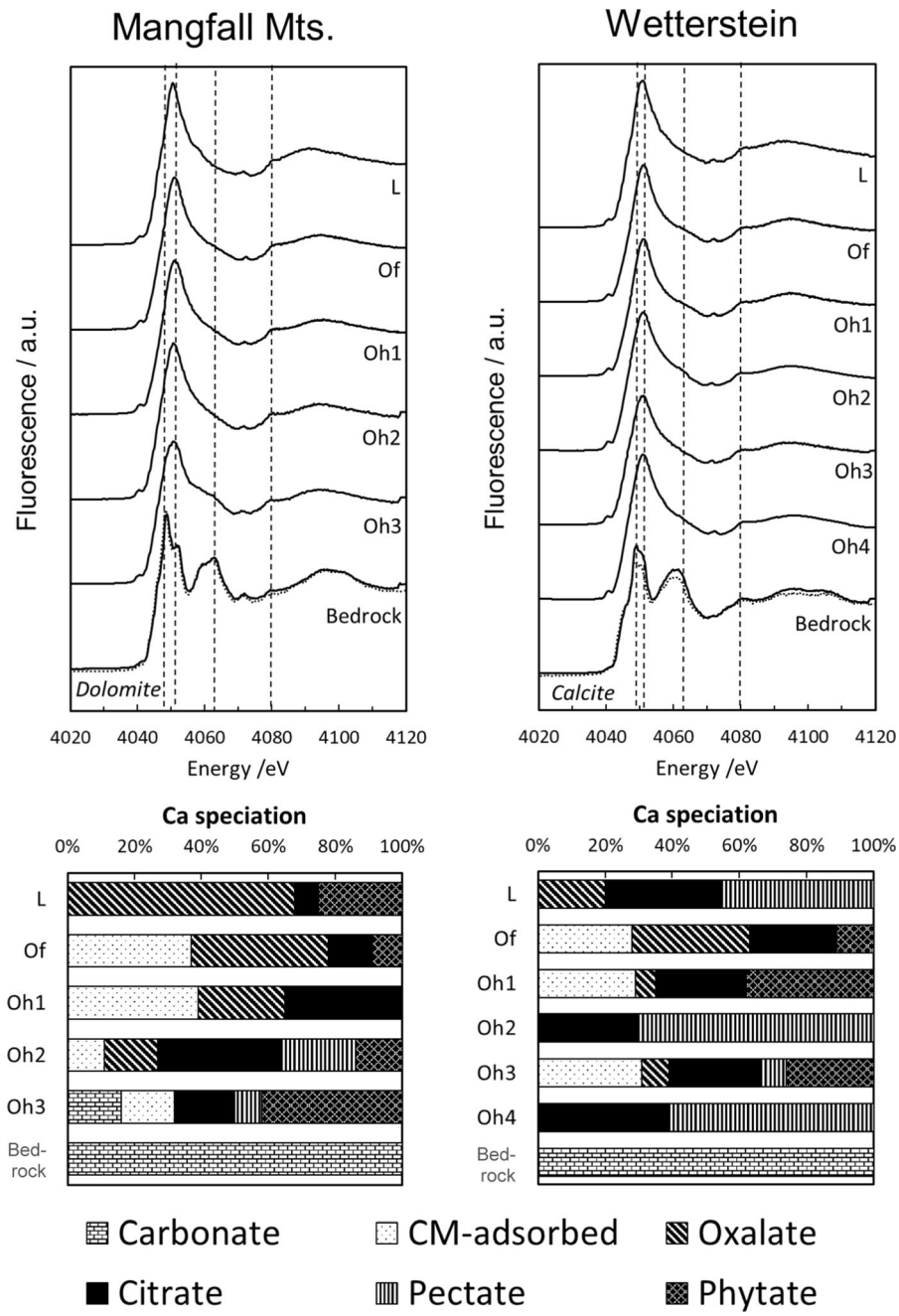


**Fig. 4** (Top panels) Normalized Ca K-edge XANES spectra and (bottom panels) contribution of different Ca species to total Ca in different horizons of Rockic Histosols (*Mangfall Mts.*, *Wetterstein*) as determined by Linear combination fitting. Ca carboxylate species other than oxalate or pectate are summarized as Ca citrate. CM: Clay mineral

**Table 6** Ca speciation in mountain soils with thick organic surface layers (Folic Histosols) on calcareous parent material and Dystric Cambisols with silicate parent material as calculated by Linear Combination Fitting performed on Ca K-edge XANES spectra of the respective samples

| Horizon | Total Ca mg $g^{-1}$ | Carbonate/ silicate Ca[a] | Clay mineral sorbed Ca | Oxalate Ca | Citrate Ca | Pectate Ca | Phytate Ca | Organic Ca/ Total Ca | Organic $Ca_{exch}$/ Total $Ca_{exch}$ | Oxalate Ca/ Organic Ca | R factor LCF |
|---|---|---|---|---|---|---|---|---|---|---|---|
| *Rockic Histosol MANGFALL MTS* | | | | | | | | | | | |
| L | 16 | 0 | 0 | 10.9 | 1 | 0 | 4 | 1.0 | ND | 0.68 | 0.000288 |
| Of | 13 | 0 | 5 | 5.3 | 2 | 0 | 1 | 0.63 | 0.53 | 0.65 | 0.002342 |
| Oh1 | 7 | 0 | 3 | 1.8 | 3 | 0 | 0 | 0.61 | 0.83 | 0.43 | 0.002887 |
| Oh2 | 11 | 0 | 1 | 1.8 | 4 | 2 | 2 | 0.89 | 0.49 | 0.18 | 0.001254 |
| Oh3 | 36 | 6 | 6 | 0.0 | 7 | 3 | 15 | 0.68 | ND | 0 | 0.000711 |
| Bedrock | 222 | 222 | 0 | 0 | 0 | 0 | 0 | 0 | | | |
| *Rockic Histosol WETTERSTEIN* | | | | | | | | | | | |
| L | 8 | 0 | 0 | 1.7 | 3 | 4 | 0 | 1.0 | ND | 0.20 | 0.005293 |
| Of | 9 | 0 | 2.4 | 3.0 | 2 | 0 | 1 | 0.72 | 0.88 | 0.49 | 0.003380 |
| Oh1 | 32 | 0 | 9.2 | 1.9 | 9 | 0 | 12 | 0.71 | 0.56 | 0.08 | 0.000981 |
| Oh2 | 37 | 0 | 0 | 0 | 11 | 26 | 0 | 1.0 | 1.0 | 0 | 0.003171 |
| Oh3 | 37 | 0 | 11 | 2.9 | 10 | 3 | 10 | 0.69 | 0.46 | 0.12 | 0.000807 |
| Oh4 | 44 | 0 | 0 | 0 | 17 | 27 | 0 | 1.0 | 1.0 | 0 | 0.007892 |
| Bedrock | 331 | 331 | 0 | 0 | 0 | 0 | 0 | 0 | | | |
| *Dystric Cambisol BAD BRÜCKENAU* | | | | | | | | | | | |
| L | 10 | 0 | 2 | 5 | 2 | 0 | 0 | 0.77 | ND | 0.69 | 0.002366 |
| Of | 9 | 0 | 3 | 3 | 3 | 0 | 0 | 0.67 | 0.52 | 0.45 | 0.002376 |
| Ah | 7 | 4 | 0 | 1 | < 1 | < 17 | 0 | 0.36 | 1.0 | 0.42 | 0.001578 |
| BwAh | 13 | 5 | 2 | 4 | 0 | 0 | < 1 | 0.44 | 0.31 | 0.84 | 0.001956 |
| Bw1 | 13 | 4 | 2 | 4 | < 1 | 0 | 3 | 0.55 | 0.56 | 0.49 | 0.001495 |
| Bw2 | 14 | 10 | 0 | 0 | 3 | 2 | 0 | 0.32 | 1.0 | 0 | 0.001138 |
| Bedrock | 69 | 69 | 0 | 0 | 0 | 0 | 0 | 0 | | | 0.000841 |
| *Dystric Cambisol STEINACH* | | | | | | | | | | | |
| LOf | 11 | 0 | 4 | 4 | 3 | < 1 | 0 | 0.68 | 0.40 | 0.47 | 0.001231 |
| Ah | 25 | 14 | 4 | 7 | 0 | 0 | 0 | 0.29 | ND | 1.0 | 0.001062 |
| Bw1 | 31 | 18 | 0 | 7 | 0 | 0 | 2 | 0.28 | ND | 0.82 | 0.000929 |
| Bw2 | 55 | 32 | 9 | 11 | 0 | 0 | 0 | 0.22 | ND | 1.0 | 0.000756 |
| Bw3 | 64 | 39 | 12 | 13 | 0 | 0 | 0 | 0.21 | ND | 1.0 | 0.000630 |

**Table 6** continued

| Horizon | Total Ca mg g$^{-1}$ | Carbonate/silicate Ca[a] | Clay mineral sorbed Ca | Oxalate Ca | Citrate Ca | Pectate Ca | Phytate Ca | Organic Ca/Total Ca | Organic $Ca_{exch}$/Total $Ca_{exch}$ | Oxalate Ca/Organic Ca | R factor LCF |
|---|---|---|---|---|---|---|---|---|---|---|---|
| CBw | 65 | 44 | 10 | 10 | 0 | 0 | 0 | 0.16 | ND | 1.0 | 0.000877 |
| Bedrock[b] | *69* | *69* | *0* | *0* | *0* | *0* | *0* | *0* | | | 0.000841 |

[a]Mangfall Mts., Wetterstein: Carbonate-Ca; Bad Brückenau, Steinach: silicate Ca

[b]*Bedrock Bad Brückenau (see Text)*

## Discussion

### Soil Ca speciation using Ca XANES spectroscopy: potential and limitations

At present, most published Ca K-edge XANES spectra of standard compounds with relevance in environmental samples refer to minerals (Neuville et al. 2004; Sarret et al. 2007; Brinza et al. 2014; Blanchard et al. 2016; Proffit et al. 2016). In contrast, XANES spectra of Ca-bearing organic standard compounds with relevance in environmental science are scarce. Sarret et al. (2007), Abe (2014), Thyrel et al. (2015), and Proffit et al. (2016) presented spectra of Ca oxalate. A comprehensive Ca K-edge XANES spectra database for relevant inorganic and organic soil Ca compounds is presented for the first time here (Table 3 and Fig. 1). The most important soil Ca species (Ca bound to SOM, carbonates, primary silicates, clay minerals, and sulfates) can be fingerprinted with reasonable reliability by LCF using our spectra database. This is in line with results of studies on minerals in mine tailings (Blanchard et al. 2016). However, a shortcoming of the deconvolution of Ca XANES spectra obtained on soil samples is the inability to account for different $Ca^{2+}$ cation bridge architectures. Soil calcium is present as the divalent cation $Ca^{2+}$, which is able to act as bridging cation between different soil constituents (Clarholm et al. 2015; Rowley et al. 2018). These constituents may either be of the same type, *e.g.* clay-mineral|–$Ca^{2+}$–|clay mineral; SOM–COO|–$Ca^{2+}$–|OOC–SOM, or of different types, e.g. clay-mineral|–$Ca^{2+}$–|OOC–SOM; Fe oxyhydroxide-$PO_4$|–$Ca^{2+}$–|OOC–SOM (Mikutta et al. 2007; Kunhi Mouvenchery et al. 2012; Clarholm and Skyllberg 2013; Rowley et al. 2018; Rasmussen et al. 2018). Simultaneous binding of a given Ca atom to two different soil constituents conflicts with our current LCF evaluation and Ca speciation scheme, where Ca always is assigned to one single specific constituent, i.e. it by definition is either present as "organically bound Ca" or as "clay mineral-bound Ca". The same problem exists for surface Ca atoms of carbonates with adsorbed SOM (Suess 1970; Carter 1978; Suzuki 2002; Rowley et al. 2018). A similar issue is the question, whether $Ca^{2+}$ ions bound to specific carboxylate groups (e.g. oxalate or citrate, which can be distinguished and quantified specifically by LCF based on spectral differences) are bound (i) as "salt" of the

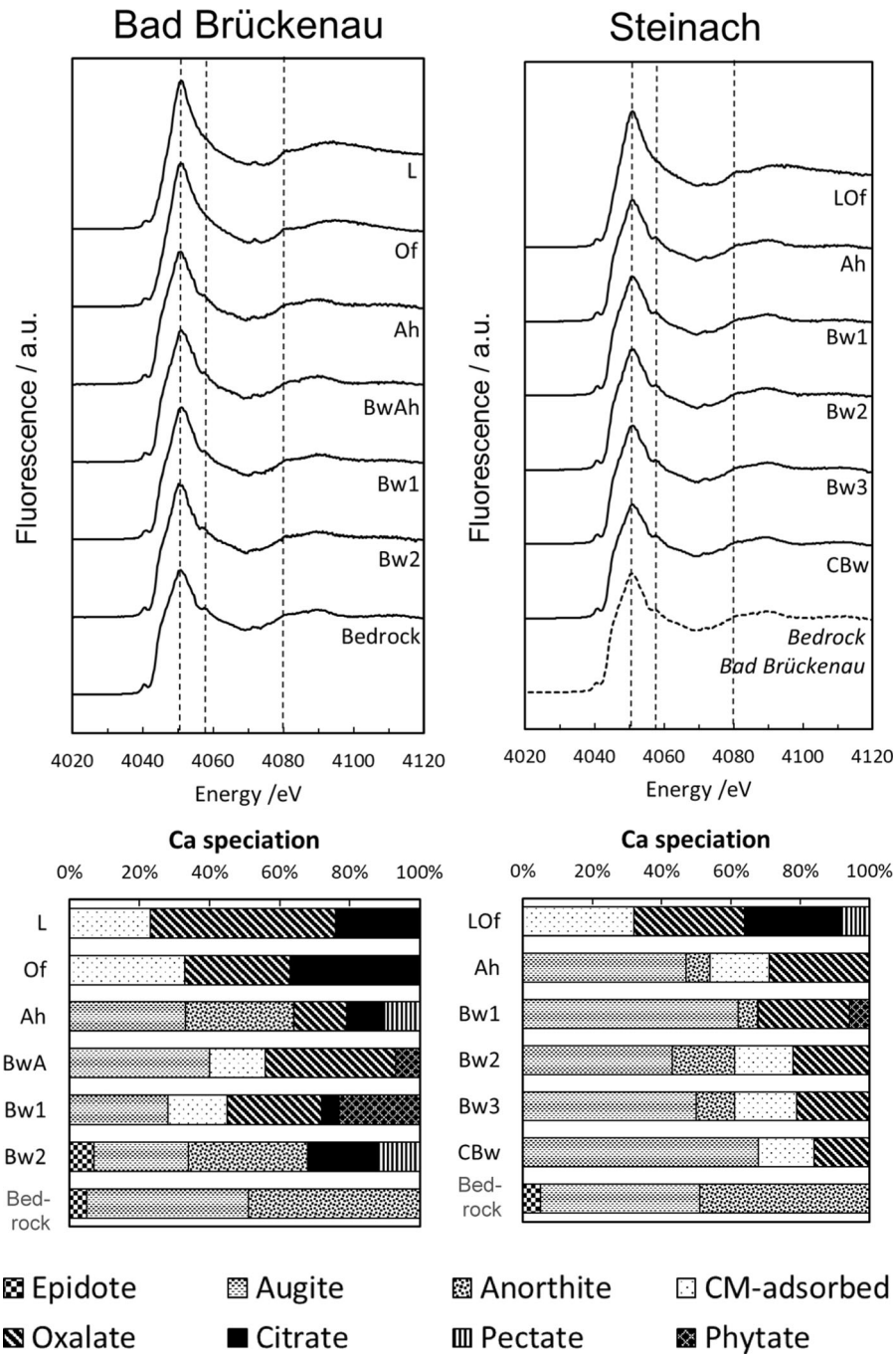


**Fig. 5** (Top panels) Normalized Ca K-edge XANES spectra and (bottom panels) contribution of different Ca species to total Ca in different horizons of Cambisols formed from Basalt (*Bad Brückenau, Steinach*) as determined by Linear combination fitting. Ca carboxylate species other than oxalate or pectate are summarized as Ca citrate. CM: Clay mineral

respective monomeric carbonic acid (e.g. oxalic acid, citric acid), or (ii) to oxalate-type *vs.* citrate-type moieties of larger SOM associations. Due to its divalence, a given $Ca^{2+}$ ion may even at the same time be bound to (iii) similar or (iv) different carboxylate-type moieties of two separate SOM

**Table 7** Ca speciation in tree foliage and fine roots sampled at the study sites as calculated by Linear Combination Fitting performed on Ca K-edge XANES spectra of the respective samples

| Sample | Location | Total Ca mg $g^{-1}$ | Oxalate Ca | Citrate Ca | Pectate Ca | Phytate Ca | Oxalate Ca/ Organic Ca | R factor LCF |
|---|---|---|---|---|---|---|---|---|
| Foliage | | | | | | | | |
| Beech | Achenpass | 13.1 | 6.7 | 0 | 4.6 | 1.8 | 0.51 | 0.0010854 |
| | Mangfall Mts | 14.2 | 7.7 | 0 | 5.3 | 1.3 | 0.55 | 0.0007346 |
| | Wellheim | 19.1 | 9.9 | 0 | 8.0 | 1.1 | 0.52 | 0.0006224 |
| Maple | Achenpass | 24.8 | 12.4 | 0 | 11.4 | 1.2 | 0.48 | 0.0010495 |
| | Mangfall Mts | 24.2 | 12.4 | 0 | 12.4 | 0 | 0.50 | 0.0005367 |
| Spruce (current-year) | Achenpass | 4.0 | 3.6 | 0.4 | 0 | 0 | 0.91 | 0.0005894 |
| Spruce (current-year) | Mangfall Mts | 4.3 | 3.7 | 0.6 | 0 | 0 | 0.86 | 0.0004622 |
| Spruce (older) | Achenpass | 6.2 | 5.5 | 0.7 | 0 | 0 | 0.88 | 0.0008229 |
| Spruce (older) | Mangfall Mts | 8.0 | 7.3 | 0.7 | 0 | 0 | 0.99 | 0.0007243 |
| Fir (current-year) | Achenpass | 3.8 | 3.6 | 0.2 | 0 | 0 | 0.94 | 0.0008700 |
| Fir (current-year) | Mangfall Mts | 5.9 | 5.3 | 0.6 | 0 | 0 | 0.90 | 0.0009893 |
| Fir (older) | Achenpass | 8.6 | 7.8 | 0.8 | 0 | 0 | 0.91 | 0.0005585 |
| Fir (older) | Mangfall Mts | 6.8 | 6.4 | 0.4 | 0 | 0 | 0.94 | 0.0006655 |
| Fine roots | | | | | | | | |
| Beech | Achenpass lleptosol | 12.3 | 2.2 | 0 | 7.3 | 2.8 | 0.23 | 0.0005481 |
| | Achenpass cambisol | 18.1 | 4.2 | 0 | 9.1 | 4.9 | 0.18 | 0.0003668 |
| | Mangfall Mts. leptosol | 10.2 | 1.9 | 0 | 5.7 | 2.6 | 0.19 | 0.0007818 |
| Spruce | Mangfall Mts. histosol | 4.2 | 1.4 | 1.1 | 1.3 | 0.4 | 0.33 | 0.0009612 |

molecules by intermolecular cross-linking (Kunhi Mouvenchery et al. 2012). Thus, our current LCF approach is a simplification of true Ca binding patterns in most soils. A possible strategy to address the problem of simultaneous binding of a given $Ca^{2+}$ ion to two different soil constituents or bonding partners in future studies may be the synthesis of appropriate reference compounds, followed by acquisition of their Ca XANES reference spectra and inclusion of these spectra in the deconvolution procedure, as performed by Prietzel et al. (2009, 2016b) for the speciation of S and P in soils by S and P XANES spectroscopy, respectively. However, this will reduce, but not eliminate the complex problem of appropriate Ca bonding partner assignment. Yet we propose that Ca XANES spectroscopy is a considerable step forward on the long road of accurate and robust soil Ca speciation. Kunhi Mouvenchery et al. (2012) recommended combination of various analytical methods including XAFS techniques for investigating Ca-mediated cross-linking between different soil components, and such combination may also help to yield most accurate soil Ca speciation results. Despite the uncertainties mentioned above, Ca speciation by XANES spectroscopy as reported for our twelve study soils with different parent material, pedogenesis, and general physicochemical properties shows good agreement with the expected Ca speciation. This underpins the validity of synchrotron-based XANES spectroscopy for the Ca speciation in soils, generating new knowledge on the fate of Ca during pedogenesis.

The quantification of different Ca species in soils and other environmental materials is a more difficult task than their identification. The correctness of LCF

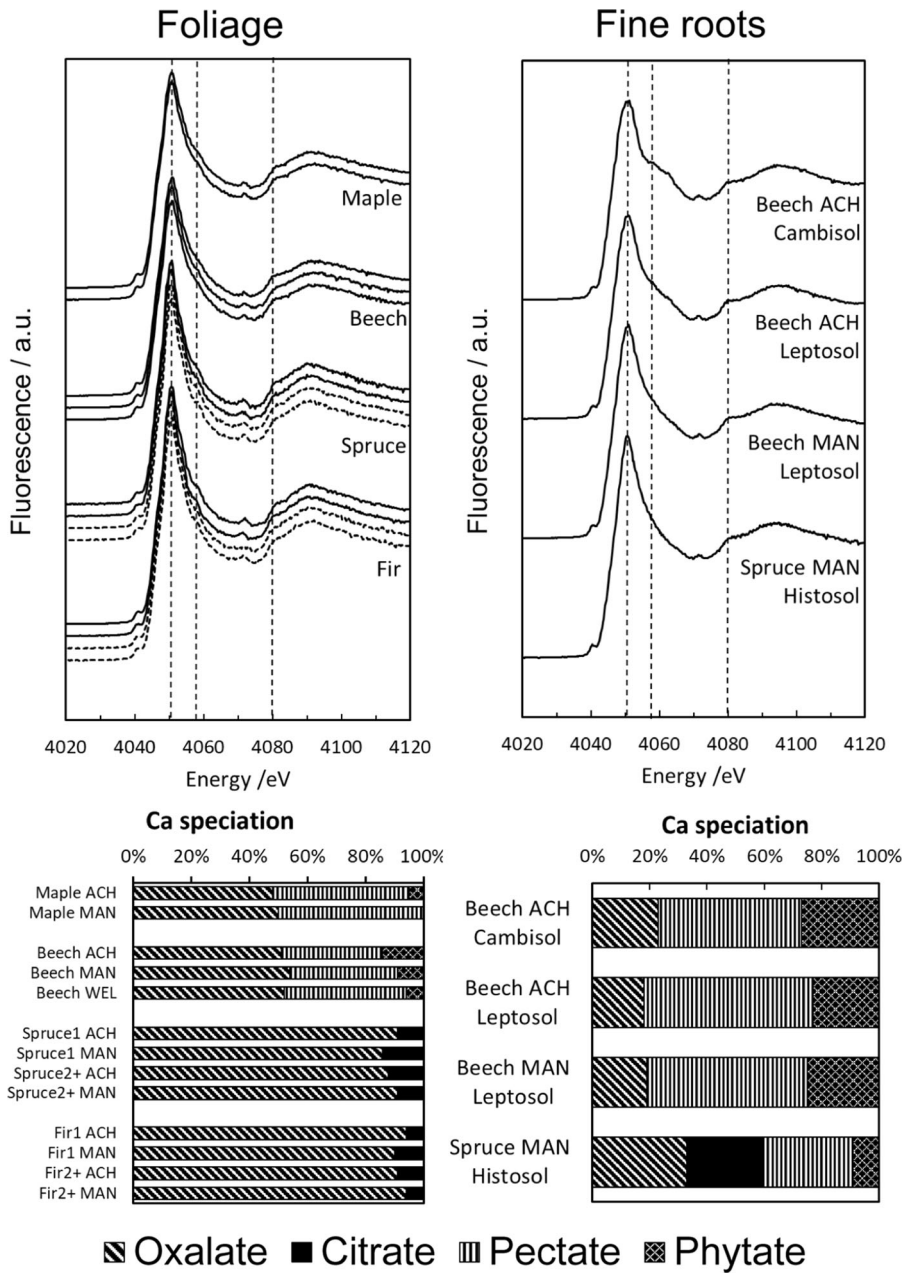


**Fig. 6** (Top panels) Normalized Ca K-edge XANES spectra and (bottom panels) contribution of different Ca species to total Ca in foliage of different tree species (left panels) and fine roots in Ah horizons of Rendzic Leptosols and Eutric Cambisols (right panels) as determined by Linear combination fitting. Ca carbyxalate species other than oxalate or pectate are summarized as Ca citrate

results (accuracy and precision of the calculated *vs.* true contribution of different species) requires (i) completeness and correctness of the reference compound set used (Kelly et al. 2008), as well as (ii) avoidance of overfitting artifacts as recently documented for P XANES speciation on soils by Gustafsson et al. (2020). Small R factors and standard errors of an LCF result do not necessarily prove a high accuracy and precision of that result, and even a high conformity of calculated speciation results with the true speciation of

well-defined mixtures (*e.g.* Prietzel et al. 2011; Werner and Prietzel 2015) does not necessarily grant a high accuracy and precision of the same procedure for soils and other environmental samples, which most often are characterized by numerous, sometimes ill-defined or even unknown species of the element under study. Combined application of different analytical methods and stoichiometric considerations may disprove or strengthen element speciation results obtained by XANES/LCF. One of the Ca species that has been quantified by XANES/LCF in our study soils, carbonate-bound Ca, can also be quantified through wet chemical analysis by calculating the concentrations of calcite and dolomite in the respective sample from the amount of inorganic (carbonate) C (Tables SI1, SI2), assuming that the carbonate is entirely bound in either calcite or dolomite depending on the site, and a Ca/carbonate C mass ratio of 40.08/12.01 and 20.04/12.01 in calcite and dolomite, respectively. Comparison of wet-chemical analysis and XANES/LCF results (Fig. 7) shows that in our study carbonate-bound Ca obviously was fairly well quantified by Ca XANES/LCF. Unfortunately, no wet-chemical method is available for quantification of the other Ca species quantified by Ca XANES/LCF in our study. On one hand, this lack emphasizes the great potential of Ca XANES to increase our knowledge on Ca in soils; on the other hand it makes it complicated to double-check the general accuracy and precision of Ca XANES spectroscopy performed on soils. Thus, our quantification results at the moment must be viewed with caution, particularly in the light of the current uncertainties with respect to the complexity of Ca binding types in soils discussed in the previous paragraph. Yet the fact that carbonate-bound Ca was fairly well quantified by Ca XANES/LCF in our study allows us to consider the Ca quantification results obtained in our study as fair estimates, being the basis for future follow up research.

## New knowledge on soil Ca speciation obtained by Ca XANES spectroscopy

### *Effects of pedogenesis on soil Ca speciation*

Our Ca speciation results obtained by XANES spectroscopy follow systematic patterns that agree well with our current knowledge on key soil formation processes in the different soil types. Thus, subsoil Ca

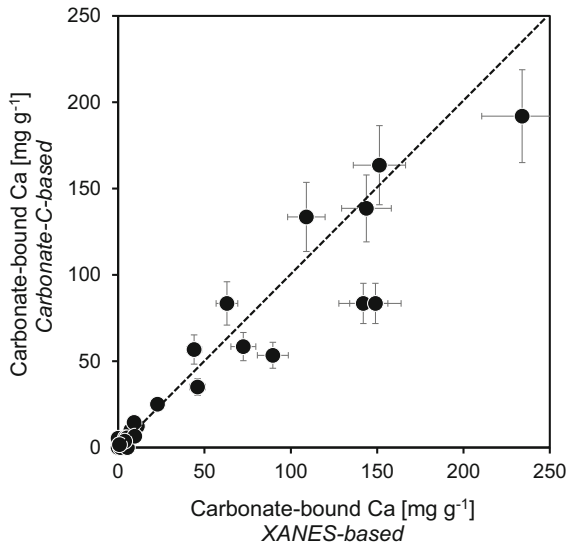


**Fig. 7** Comparison of carbonate-bound Ca in the study soils as calculated by Ca K-edge XANES + LCF and by wet chemical analysis based on the concentration of inorganic (= carbonate) carbon. Error range estimated as 10% for XANES, Ca and carbonate determination, respectively

in the Rendzic Leptosols was identified as lithogenic carbonate. Topsoil Ca concentrations were decreased markedly compared to those in the subsoil due to carbonate weathering. Concomitantly with increased topsoil contents of Fe/Al oxyhydroxides and SOM (Table S1) due to intensive mineral weathering, pedogenesis, and biotic activity, also concentrations of organically bound Ca and clay mineral-adsorbed Ca (Table 4), and therefore the relative contributions of these Ca forms to total soil Ca were larger in topsoil than subsoil horizons. Our XANES approach additionally showed that the four Rendzic Leptosols differ with respect to their topsoil Ca speciation. This can be explained by site-specific pedogenesis and SOC contents. The decreasing contribution of carbonate-bound Ca in the Leptosol Ah horizons in the sequence *Achenpass* > *Wellheim* > *Mangfall Mts.* > *Tuttlingen* reflects the progressively advanced stage of pedogenesis in these soils. The topsoil of *Tuttlingen* is most depleted in Ca (Table 4) and has almost completely lost its carbonate (Table S1). Intensive limestone weathering has resulted in pronounced Al/Fe oxyhydroxide and clay mineral accumulation, which together with SOM (cf. "Speciation of organically bound soil Ca as affected by plant input and microbial turnover" sect.) act as effective $Ca^{2+}$

sorbents. The mineral topsoil of the *Mangfall Mts.* Leptosol is much richer in Ca and carbonate, but also shows marked Al/Fe oxyhydroxide accumulation. This soil profile is located on a steep (30°) N-exposed slope and characterized by intensive carbonate weathering and sesquioxide formation together with continuous input of dolomite scree from topslope rock walls. This results in the presence of about equal shares of carbonate-bound Ca, organically bound Ca, and clay mineral-bound Ca in the Ah horizon. *Achenpass* is the least developed Leptosol and characterized by large Ca and carbonate contents as well as small SOM and Al/Fe oxyhydroxide contents in the Ah horizon. Consequently, its Ca speciation shows a predominance of carbonate-bound Ca.

In agreement with traditional concepts of pedogenesis on carbonate parent material, the Eutric Cambisols at the calcareous sites differ from their Leptosol counterparts by complete disappearance (*Tuttlingen*; *Wellheim*) or decreased contents (*Achenpass; Mangfall Mts*.) of carbonate-bound Ca, and accumulation of organically bound and clay mineral-bound Ca in the topsoil (Table 5). Additionally, different depth gradients of carbonate-bound Ca, total Ca, inorganic C, and pH were noticed for the non-alpine Cambisols *Tuttlingen* and *Wellheim* on one hand and the alpine Cambisols *Achenpass* and *Mangfall Mts*. on the other, providing important hints for peculiar patterns of pedogenesis in the latter soils. In this context it must be mentioned that the latter soils both are located at midslope positions of steep hillslopes with upslope rock outcrops and rock walls consisting of dolostone. Physical dolostone weathering and downslope transport of mobilized dolostone fragments by gravity and snow gliding result in continuous input of dolomite scree on the soil surface and its subsequent admixture into the topsoil by bioturbation. Continuous topsoil dolomite scree input together with the cool and humid climate at sites *Achenpass* and *Mangfall Mts*. (Table 2) results in intensive carbonate weathering and pedogenesis, allowing the formation of Cambisol Bw horizons within only 10,000 years of Holocene pedogenesis (Biermayer and Rehfuess 1985). In contrast to the Cambisols *Tuttlingen* and *Wellheim* which lack upslope rock outcrops or walls and thus any topsoil input of unweathered parent material, the Cambisols *Achenpass* and *Mangfall Mts*. have two different zones with intensive carbonate weathering and soil formation, one in the Ah horizon (input of allochtonous carbonate) and another in the BC and C horizons (autochtonous carbonate). In the Ah, BC, and C horizons, soil pH is controlled by carbonate weathering, whereas the de-carbonated Bw horizons are characterized by intensive silicate weathering. To the best of our knowledge, this "double pedogenesis" in Cambisols on calcareous hillslopes with superficial input of chemically unweathered calcareous fragments has not been described before, but could be clearly identified in our Ca XANES study.

As shown by comparison of the Eutric Cambisols, weathering intensity strongly affects the amount of clay mineral-bound Ca. This is mainly due to the fact that with progressive pedogenesis and topsoil acidification clay mineral-adsorbed topsoil Ca is increasingly replaced by Al cations, as evident in decreased topsoil base saturation percentages for the Cambisols *Wellheim* and *Tuttlingen* (Table S2). Additionally, total CEC in the Bw horizons of the *Wellheim* and *Tuttlingen* Cambisols, Table S2) is much smaller compared to those of the Cambisols *Achenpass* and *Mangfall Mts.* despite large clay contents. This is due to the fact, that pedogenesis of the *Wellheim* and *Tuttlingen* Cambisols started in the Tertiary (2.5–65 million years ago), whereas pedogenesis of the Cambisols *Achenpass* and *Mangfall Mts.* started in the Holocene (< 12,000 years). Therefore, soil development is considerably advanced in the former ($Fe_d$/$Fe_o$ ratio in B and CB horizons: 16–115; dominating clay mineral: kaolinite; Stahr and Böcker 2014) compared to the latter soils ($Fe_d$/$Fe_o$ ratio in B and CB horizons: 3–6; dominating clay minerals: illite and smectite; Wilke et al. 1984; Biermayer and Rehfuess 1985). Compared to the Cambisols formed from calcareous bedrock, in the Dystric Cambisols *Bad Brückenau* and *Steinach* that have developed from silicate bedrock (basalt), a considerably larger part of mineral soil Ca is bound as primary silicate Ca in the fine earth and rock fragments < 2 mm diameter. This underlines the importance of lithogenic Ca for Ca nutrition of temperate forest ecosystems with soils on silicate bedrock (Kohler et al. 2000).

Our study shows that pedogenesis in temperate forest soils results in soil Ca speciation changes from lithogenic Ca to lithogenic + organically bound Ca forms and ultimately to clay mineral-bound Ca and/or organically bound Ca forms. This process starts in the topsoil and advances into the subsoil with progressive pedogenesis. For the first time ever, we synthesized

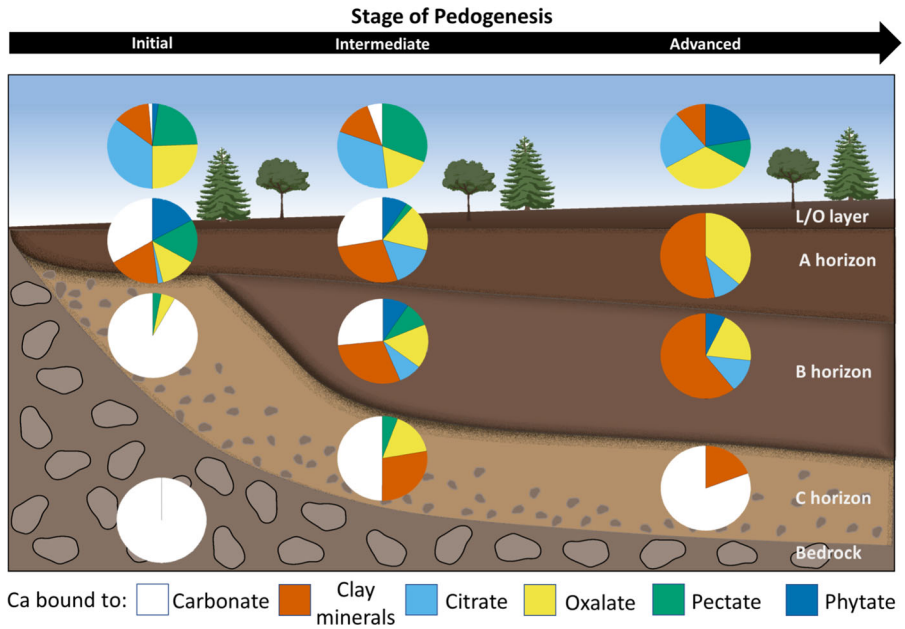


**Fig. 8** Conceptual model of Ca speciation change in temperate forest soils on calcareous bedrock during pedogenesis. In our study, the Rendzic Leptosols, the Eutric Cambisols (except *Tuttlingen*), and the Eutric Cambisol *Tuttlingen,* respectively, represent soils with initial, intermediate, and advanced stage of pedogenesis

these processes in a conceptual model of Ca speciation change in temperate soils on calcareous bedrock during pedogenesis (Fig. 8). As noted in the previous paragraph, continuous superficial input of unweathered Ca carbonate may modify the pattern of soil Ca speciation change during pedogenesis. Similar patterns as those depicted in Fig. 8 for calcareous soils can also be expected for soils on silicate bedrock; however, in our study only silicate-derived soils with an intermediate stage of pedogenesis (Dystric Cambisols) and particularly large lithogenic Ca contents (parent bedrock: basalt) have been investigated. Future follow-up studies on the effect of pedogenesis on soil Ca speciation should therefore also include initial soils on silicate bedrock (Regosols, Leptosols), soils on silicate bedrock with advanced pedogenesis, and additionally also soils formed on silicate bedrock with small Ca contents (granite, gneiss) in order to yield a more generalized picture of Ca speciation changes in temperate forest soils during pedogenesis.

### *Speciation of organically bound soil Ca as affected by plant input and microbial turnover*

Organically bound Ca enters the forest floor surface via litter fall (foliage, seeds, twigs, bark particles) deposited on and being converted into L layers and by root necromass injection into Of and Oh layers. In rooted horizons of high-base-saturation soils, Ca oxalate additionally is formed in situ by reaction of (mycor) rhizogenic oxalic acid with $Ca^{2+}$ cations (Clarholm et al. 2015). The Ca speciation in the L layers of the Leptosols and Cambisols was dominated by Ca pectate and Ca oxalate and almost identical with that of beech foliage, which is the dominating litter source at the respective sites. In contrast to spruce, fir, and maple, beech seems to accumulate a significant P amount in its foliage as Ca phytate (Fig. 6). However, L layer Ca speciation differs from beech leaf Ca speciation by the absence of phytate-bound Ca, indicating rapid decomposition of Ca phytate after litter deposition. For the *Mangfall. Mts.* Histosol, L layer Ca speciation reflected the input of spruce and beech litter. Progressive aging and microbial decomposition of forest floor SOM from L to Of and Oh layers is associated with a marked decrease of the

contribution of oxalate-bound Ca to organically-bound Ca in all Leptosols and Histosols. Oxalate-bound Ca is completely absent in lower, older sections (Oh3, Oh4) of the thick Rockic Histosol O layers (Fig. 4) and also in most mineral soil horizons of the Rendzic Leptosols (Fig. 2) as well as in the B and BC horizons of the Eutric Cambisols (Fig. 5). O layer Ca speciation also differs between the Histosols *Mangfall Mts.* (SOM radiocarbon age in Oh3 horizon: 160 years; organically bound Ca largely present as phytate and citrate) and *Wetterstein* (SOM radiocarbon age in Oh4 horizon: 1560 years; organically bound Ca largely present as pectate and phytate). Whereas > 30% of spruce fine root Ca in the *Mangfall Mts.* Histosol is oxalate-bound (Fig. 6), the contribution of oxalate-bound Ca to organically bound Ca in the Oh2 horizon of that Histosol is < 20% and in the Oh3 horizon < 5%. Thus, Ca oxalate, may its origin be foliage, root litter, or (mycor)rhizogenic oxalic acid, obviously is decomposed rapidly compared to Ca pectate or Ca citrate in the Histosols during long-term O layer ageing (up to 150 years at *Mangfall Mts.* and 1500 years at *Wetterstein*). Ca phytate was not only identified as major soil Ca form in both Histosols, but also as major P form by P XANES and NMR spectroscopy in the *Wetterstein* Histosol (Wang et al. 2019) and in the Leptosols (Prietzel et al. 2016a).

*The fate of Ca oxalate in calcareous and silicate soils*

Calcium oxalate plays an important role for the growth and metabolism of most terrestrial plants (Franceschi and Nakata 2005). Calcium is taken up passively by plant roots and transported with the transpiration water stream from the roots through the xylem to the foliage, deposited as Ca oxalate in cell walls and foliage cell vacuoles if present in excess to the amount needed as nutrient, and ultimately disposed by leaf shedding (Marschner 1995; Franceschi and Nakata 2005). Synthesis of Ca oxalate and its subsequent deposition in plant foliage vacuoles besides protection against herbivory allows terrestrial plants maintaining water uptake and photosynthesis also at sites with elevated soil solution Ca concentrations without costly Ca discrimination at soil–root interfaces (Marschner 1995; Franceschi and Nakata 2005). This process is particularly intensive for broadleaf trees (e.g. *Fagus sylvatica;, Acer spp.*) which are characterized by large stomatal conductance and large foliar Ca concentrations (Table 7), and an important factor enhancing growth competitiveness of these species on calcareous sites. Even though oxalate-bound Ca comprises a smaller proportion of total Ca in broadleaf compared to the conifer foliage (Fig. 6), foliar Ca oxalate concentrations (Table 7) as well annual litter fall amounts (Vesterdal et al. 2008), and thus the annual litter fall input of oxalate-bound Ca to soils are probably similar for broadleaf and conifer species. Thus, photosynthetic $CO_2$ fixation by trees leads to a considerable flux of Ca oxalate into forest soils (Verrecchia et al. 2006; Cailleau et al. 2004, 2005), and large Ca oxalate concentrations in forest soil litter layers have already been reported by Graustein et al. (1977). Together with the input of Ca pectate by foliage deposition and fine root necromass injection into topsoil horizons, Ca oxalate deposition on soil surfaces via litter fall is a major component of the "base pumping effect" of forest trees, since oxalate-bound Ca can make up to 90% of total plant tissue Ca (Franceschi and Nakata, 2005; our study: 50% of total Ca in broadleaf foliage and 90% in conifer foliage; Fig. 6). This effect results in elevated Ca concentrations also in O layers of forest soils with advanced mineral topsoil acidification and Ca depletion (Clarholm and Skyllberg 2013). In our study, the relevance of Ca oxalate for the Ca input into forest soils via litter fall is highlighted by markedly elevated concentrations of oxalate-bound Ca in L layers compared to deeper horizons. The decreasing contribution of Ca oxalate to total organically bound Ca with increasing soil depth in the Leptosols and Histosols despite in situ Ca oxalate synthesis by reaction of (mycor) rhizogenic oxalic acid with $Ca^{2+}$ cations (Clarholm et al. 2015) can be explained by input of Ca oxalate-poor, Ca pectate-rich root litter and microbial Ca oxalate decomposition (Sun et al. 2019). The absence of Ca oxalate in most carbonate-containing mineral soil horizons (Rendzic Leptosols, lower B and BC horizons of Eutric Cambisols) as identified by Ca XANES spectroscopy in our study at first glance is surprising. Soil fungi subject to high soil solution Ca concentrations as present in calcareous soils are known to mitigate Ca stress by synthesis of sparsely soluble Ca oxalate (Cromack et al. 1977; Graustein et al. 1977; Lapeyrie 1988; Tuason and Arocena 2009; Bindschedler et al. 2016). Moreover, plant roots and mycorrhiza fungi in calcareous soils also excrete oxalic acid (Fox and Comerford 1990; Sun et al. 2019)

in order to acquire nutrients, e.g. P from accessory apatite (Wallander 2000; Ström et al. 2005) in calcareous bedrock by enhancing carbonate weathering through proton attack and chelate complexation of Ca (Bravo et al. 2013). In line with the absence of Ca oxalate in calcareous soil horizons in our study, Messini and Favilli (1990) and Guggiari et al. (2011) reported rapid microbial Ca oxalate decomposition in such horizons. According to Verrecchia (1990) and Sun et al. (2019), the "oxalate-carbonate pathway", involving microbial Ca oxalate decomposition and production of secondary carbonate, is important for the sequestration of atmospheric $CO_2$ in calcareous soils; at the same time the scarce nutrient P is efficiently extracted from lithogenic carbonate (Wallander 2000). Our XANES results support this hypothesis and corroborate the important role of Ca oxalate for the turnover of Ca and SOM in calcareous soils.

In contrast to the calcareous soils, oxalate-bound Ca was enriched in the subsoil of the Dystric Cambisols developed on basalt, and a large portion of the organic Ca in most mineral soil horizons was oxalate-bound (Table 6 and Fig. 6). Oxalate-bound Ca in deep subsoil horizons has neither been transported there by bioturbation nor by seepage water transport, because Ca oxalate and most other Ca (poly)carboxylates are sparsely water-soluble. Rather, the Ca oxalate must have been synthesized in situ by reaction of biogenic oxalic acid (plant root and microbial exudates) with soil solution $Ca^{2+}$ (Clarholm et al. 2015) and protected against decomposition by association with pedogenic minerals (adsorption via ternary complex formation and/or occlusion; Parfitt et al. 1977a, b; Fein and Hestrin 1994; Sowers et al. 2018a, b).

### *Differentiation of organically and inorganically bound exchangeable soil Ca*

Classical methods for determination of exchangeable, plant-available cations in soils, such as extraction with $NH_4Cl$, $NH_4$ acetate, or buffered $BaCl_2$ solution do not distinguish between cations adsorbed to inorganic (e.g. clay minerals) *vs.* organic (SOM) soil constituents. However, discrimination of mineral-adsorbed *vs.* SOM-adsorbed cations may be desirable e.g. for the assessment of cation mobilization or CEC decrease risks associated with SOM losses due to climate or land-use change. Calcium K-edge XANES spectroscopy offers the possibility for semi-quantification of exchangeable $Ca^{2+}$ adsorbed to (clay) minerals and SOM, respectively. $Ca^{2+}$ cations are adsorbed to clay minerals by retaining at least part of their hydration shell (outer-sphere interaction) and thus are fully exchangeable whereas carboxylate-bound Ca is bound by both outer-sphere and inner-sphere interaction, and thus only partly exchangeable (Rowley et al. 2018). The combination of traditional wet-chemical analysis of total exchangeable $Ca^{2+}$ in a soil horizon by extraction (data for study soils: Table S1) with Ca XANES results on clay mineral-bound Ca (Tables 4, 5 and 6) allows the attribution of exchangeable Ca to either inorganic (clay minerals) or organic (SOM) Ca sorbents, assuming that the clay mineral-bound Ca is fully exchangeable and that the difference between total exchangeable Ca and clay mineral-adsorbed Ca represents organically bound exchangeable Ca.

Partitioning of total exchangeable $Ca^{2+}$ to organic *vs.* mineral sorbents differed among soil types. For the Leptosols, Histosols, and the Dystric Cambisol *Bad Brückenau*, the majority of exchangeable Ca was organically bound in the entire profile, and no depth trend of the $Ca_{exch\ organic}/Ca_{exch\ inorganic}$ ratio existed (Tables 4 and 6). This pattern can be expected for the initial and/or SOM-rich Leptosols and Histosols. The dominance of organically over inorganically bound exchangeable Ca in the subsoil of the clay- and sesquioxide-rich Cambisol *Bad Brückenau* may be due to its low pH value (4.0–4.2; Table S1). In this pH range, $Al^{3+}$ and $Al_2(OH)_2^{4+}$ cations strongly dominate over $Ca^{2+}$ in the soil solution and on cation-exchanging clay mineral surfaces, whereas $Ca^{2+}$ is bound more effectively than Al cations to SOM (Barak 1989) in the subsoil horizons of *Bad Brückenau* and particularly to oxalate adsorbed on abundant pedogenic Fe and Al oxyhydroxide surfaces (Fein and Hestrin 1994).

In both Histosols, according to XANES results up to 40% of total Ca was adsorbed to clay minerals. The organic surface horizons have accrued slowly over a long-term period (up to > 160 years at *Mangfall Mts.* and > 1500 years at *Wetterstein*), and accrual was accompanied by continuous Aeolian silicate dust deposition (Küfmann 2006; Prietzel et al. 2015). Oh layers at *Wetterstein* had OC concentrations between 207 and 342 mg $g^{-1}$ (Table S1), and thus consisted of 30–60% mineral constituents. This explains the large

contribution of clay mineral-bound Ca to total Ca in these horizons. However, this explanation is not plausible for the *Mangfall Mts.* Histosol (Oh layers with $> 460$ mg OC $g^{-1}$). The LCF results obtained for these horizons are probably impaired by methodological problems associated with the bridging cation function of $Ca^{2+}$ between SOM and clay minerals (Mikutta et al. 2007; Clarholm and Skyllberg 2013) described in "Soil Ca speciation using Ca XANES spectroscopy: potential and limitations" sect.

Outlook

As mentioned above, synthesis of Ca reference compounds characterized by simultaneous bonding of $Ca^{2+}$ to different soil constituents (e.g. minerals and SOM) and their inclusion in spectrum deconvolution protocols will help to increase the accuracy of Ca speciation results based on XANES spectroscopy. Moreover, Ca XANES spectra obtained in fluorescence mode have a good signal-to-noise ratio for samples with Ca concentrations of 1 mg $g^{-1}$ (Figure S3) and probably also below, making the method suitable for the Ca speciation of soils with low Ca concentrations. Future applications of Ca XANES spectroscopy in soil science and forest ecology may include (i) tracing the turnover and speciation changes of Ca applied to soils by liming (Huber et al. 2006) or Ca fertilization (Cho et al. 2012), including effects on forest trees (Halman et al. 2008), (ii) studies on the reactivity of Ca in binary and ternary mineral–SOM–Ca complexes (Rasmussen et al. 2018; Adhikari et al. 2019), and (iii) investigation of the role of $Ca^{2+}$ in soil aggregation (Gaiffe et al. 1984) and SOM stabilization (Rasmussen et al. 2018). Moreover, Ca XANES spectroscopy may help in elucidation of Ca cycling in forest soils and ecosystems (Likens et al. 1998; Yanai et al. 2005), and watersheds (Kirchner and Lydersen 1995; Likens et al. 1998; Cho et al. 2012). More specifically, Ca XANES spectroscopy may be a promising tool for studies investigating Ca-depleting effects of acid rain and forest ageing (e.g. DeHayes et al. 1999; Hamburg et al. 2003; Yanai et al. 2005), effects of ecosystem recovery characterized by an improving soil Ca status and tree Ca supply after acid deposition decrease (Prietzel et al. 2020a), or effects of stand regeneration (Yanai et al. 2005). Together with P XANES spectroscopy (Prietzel et al. 2016a), Ca XANES spectroscopy may also contribute to reveal the role of apatite for Ca nutrition of trees and forest ecosystems on different silicate bedrock types (Blum et al. 2002; Yanai et al. 2005). In summary, synchrotron-based Ca XANES spectroscopy—particularly when applied at (sub)micron scale (μ-XANES; μ-XRF) and/or combined with other techniques (e.g. density fractionation; Sollins et al. 2009; Prietzel et al. 2020b)—is a promising novel tool to study the versatile functions of Ca in soils and terrestrial ecosystems.

## Conclusions

- Synchrotron-based Ca K-edge XANES spectroscopy allows the speciation of different Ca forms in soils and other environmental samples and to reveal the fate of soil Ca during biogeochemical turnover and pedogenesis.
- In temperate forest soils, pedogenesis results in Ca speciation change from lithogenic Ca to lithogenic + organically bound forms and ultimately to clay mineral-bound Ca and/or organically bound Ca forms. A conceptual model of Ca speciation change in temperate soils on calcareous bedrock during pedogenesis has been developed and is depicted in Fig. 8. Soil Ca speciation changes as identified by XANES are in line with soil chemical data obtained by traditional methods.
- Ca oxalate and Ca pectate are relevant Ca forms in forest soils. Plant-synthesized Ca oxalate is rapidly decomposed in calcareous soils but stabilized in silicate soils, probably by association with pedogenic Al and Fe minerals.
- Our approach of soil Ca speciation by XANES assigns each soil Ca atom to one of several species. However, $Ca^{2+}$ can simultaneously be bound to different soil compounds (e.g. minerals and SOM). This property is not properly addressed in our spectrum deconvolution method and requires methodological improvement.
- Synchrotron-based Ca XANES spectroscopy is a promising novel tool to study the versatile functions of Ca in soil ecology.

**Acknowledgements** The study was supported by the BLE Waldklimafonds as part of the ALPENHUMUS project. (Grant 28WC406301). The authors appreciate the assistance of Sigrid

Hiesch and Christine Pfab during sample and reference compound preparation. We want to thank the team at Beamline 8 of SLRI, Maximilian Prietzel, and Katharina Prietzel for assistance during XANES measurements. Additionally, we are grateful to Dr Klaus Kaiser, University of Halle, for providing data on CEC, exchangeable Ca, dithionite- and oxalate-extractable Fe, Al and Prof. Dr. Jan Siemens, University of Giessen, for providing data on carbonate concentrations in the study soils.



**Funding** Open Access funding enabled and organized by Projekt DEAL.

## References

Abe H (2014) Direct evidence of calcium oxalate formation in spinach. Chem Lett 43:1841–1842. https://doi.org/10.1246/cl.140726

Adhikari D, Sowers T, Stuckey JW, Wang X, Sparks DL, Yang Y (2019) Formation and redox reactivity of ferrihydrite-organic carbon-calcium co-precipitates. Geochim Cosmochim Acta 244:86–98. https://doi.org/10.1016/j.gca.2018.09.026

Andersson KO, Tighe MK, Guppy CN, Milham PJ, McLaren TI, Schefe CR, Lombi E (2016) XANES demonstrates the release of calcium phosphates from alkaline Vertisols to moderately acidified solution. Environ Sci Technol 50:4229–4237. https://doi.org/10.1021/acs.est.5b04814

Baldock JA, Skjemstad JO (2000) Role of the soil matrix and minerals in protecting natural organic materials against biological attack. Org Geochem 31:697–710. https://doi.org/10.1016/S0146-6380(00)00049-8

Barak P (1989) Double layer theory prediction of Al-Ca exchange on clay and soil. J Colloid Interf Sci 133:479–490. https://doi.org/10.1016/S0021-9797(89)80059-1

Biermayer G, Rehfuess KE (1985) Holozäne Terrae fuscae aus Carbonatgesteinen in den Nördlichen Kalkalpen. Z Pflanzenern Bodenkde 148:405–416. https://doi.org/10.1002/jpln.19851480405

Bindschedler S, Cailleau G, Verrecchia E (2016) Role of fungi in the biomineralization of calcite. Minerals 6:41. https://doi.org/10.3390/min6020041

Blanchard PER, Grosvenor AP, Rowson J, Hughes K, Brown C (2016) Identifying calcium-containing mineral species in the JEB Tailings Management Facility at McClean Lake, Saskatchewan. Appl Geochem 73:98–108. https://doi.org/10.1016/j.apgeochem.2016.08.001

Blum JD, Klaue A, Nezat CA, Driscoll CT, Johnson CE, Siccama TG, Eager C, Fahey TJ, Likens GE (2002) Mycorrhizal weathering of apatite as an important calcium source in base-poor forest ecosystems. Nature 417:729–731. https://doi.org/10.1038/nature00793

Bravo D, Martin G, David MM et al (2013) Identification of active oxalotrophic bacteria by Bromodeoxyuridine DNA labeling in a microcosm soil experiment. FEMS Microbiol Lett 348:103–111. https://doi.org/10.1111/1574-6968.12244

Briedis C, de Moraes Sá JC, Caires EF et al (2012) Soil organic matter pools and carbon-protection mechanisms in aggregate classes influenced by surface liming in a no-till system. Geoderma 170:80–88. https://doi.org/10.1016/j.geoderma.2011.10.011

Brinza L, Schofield PF, Hodson ME et al (2014) Combining μXANES and μXRD mapping to analyse the heterogeneity in calcium carbonate granules excreted by the earthworm *Lumbricus terrestris*. J Synchrotron Radiat 21:235–241. https://doi.org/10.1107/S160057751303083X

Cailleau G, Braissant O, Dupraz C, Aragno M, Verrecchia EP (2005) Biologically induced accumulations of $CaCO_3$ in orthox soils of Biga, Ivory Coast. CATENA 59:1–17. https://doi.org/10.1016/j.catena.2004.06.002

Cailleau G, Braissant O, Verrecchia EP (2004) Biomineralization in plants as a long-term carbon sink. Naturwissensch 91:191–194. https://doi.org/10.1007/s00114-004-0512-1

Carter P (1978) Adsorption of amino acid-containing organic matter by calcite and quartz. Geochim Cosmochim Acta 42:1239–1242. https://doi.org/10.1016/0016-7037(78)90117-5

Castells E, Penuelas J (2003) Is there a feedback between N availability in siliceous and calcareous soils and *Cistus albidus* leaf chemical composition? Oecologia 136:183–192. https://doi.org/10.1007/s00442-003-1258-8

Cho Y, Driscoll CT, Johnson CE et al (2012) Watershed-level responses to calcium silicate treatment in a Northern hardwood forest. Ecosystems 15:416–434. https://doi.org/10.1007/s10021-012-9518-2

Clarholm M, Skyllberg U (2013) Translocation of metals by trees and fungi regulates pH, soil organic matter turnover and nitrogen availability in acidic forest soils. Soil Biol Biochem 63:142–153. https://doi.org/10.1016/j.soilbio.2013.03.019

Clarholm M, Skyllberg U, Rosling A (2015) Organic acid induced release of nutrients from metal-stabilized soil organic matter–the unbutton model. Soil Biol Biochem 84:168–176. https://doi.org/10.1016/j.soilbio.2015.02.019

Cromack K Jr, Sollins P, Todd RL et al (1977) The role of oxalic acid and bicarbonate in calcium cycling by fungi and bacteria: some possible implications for soil animals. Ecol Bull 25:246–252

de Kerchove AJ, Elimelech M (2007) Formation of polysaccharide gel layers in the presence of $Ca^{2+}$ and $K^{+}$ ions: measurements and mechanisms. Biomacromol 8:113–121. https://doi.org/10.1021/bm060670i

DeHayes DH, Schaberg PG, Hawley GJ, Strimbeck GR (1999) Acid rain impacts on calcium nutrition and forest health. Bioscience 49:789–800. https://doi.org/10.2307/1313570

Fein JB, Hestrin JE (1994) Experimental studies of oxalate complexation at 80 °C: Gibbsite, amorphous silica, and quartz solubilities in oxalate-bearing fluids. Geochim Cosmochim Acta 58:4817–4829. https://doi.org/10.1016/0016-7037(94)90213-5

Fendorf SE, Sparks DL, Lamble GM, Kelley MJ (1994) Applications of X-ray absorption fine structure spectroscopy to soils. Soil Sci Soc Am J 58:1583–1595. https://doi.org/10.2136/sssaj1994.03615995005800060001x

Fernández-Ugalde O, Virto I, Barré P et al (2011) Effect of carbonates on the hierarchical model of aggregation in calcareous semi-arid Mediterranean soils. Geoderma 164:203–214. https://doi.org/10.1016/j.geoderma.2011.06.008

Fox TR, Comerford NB (1990) Low-molecular-weight organic acids in selected forest soils of the southeastern USA. Soil Sci Soc Am J 54:1139–1144. https://doi.org/10.2136/sssaj1990.03615995005400040037x

Franceschi VR, Nakata PA (2005) Calcium oxalate in plants: formation and function. Annu Rev Plant Biol 56:41–71. https://doi.org/10.1146/annurev.arplant.56.032604.144106

Gaiffe M, Duquet B, Tavant H, Tavant Y, Bruckert S (1984) Biological stability and physical behavior of an argillo-humic complex placed under different conditions of saturation with calcium or potassium. Plant Soil 77:271–284. https://doi.org/10.1007/BF02182930

Graustein WC, Cromack K Jr, Sollins P (1977) Calcium oxalate: occurrence in soils and effect on nutrient and geochemical cycles. Science 198:1252–1254. https://doi.org/10.1126/science.198.4323.1252

Grünewald G, Kaiser K, Jahn R, Guggenberger G (2006) Organic matter stabilization in young calcareous soils as revealed by density fractionation and analysis of lignin derived constituents. Org Geochem 37:1573–1589. https://doi.org/10.1016/j.orggeochem.2006.05.002

Guggiari M, Bloque R, Aragno M, Verrecchia E, Job D, Junier P (2011) Experimental calcium-oxalate crystal production and dissolution by selected wood-rot fungi. Intern Biodeterior Biodegrad 65:803–809. https://doi.org/10.1016/j.ibiod.2011.02.012

Gustafsson JP, Braun S, Tuyishime MJR, Adediran GA, Warrinier R, Hesterberg D (2020) A probabilistic approach to phosphorus speciation of soils using P K-edge XANES spectroscopy with linear combination fitting. Soil Syst 4:26. https://doi.org/10.3390/soilsystems4020026

Halman JM, Schaberg PG, Hawley GJ, Eagar C (2008) Calcium addition at the Hubbard Brook Experimental Forest increases sugar storage, antioxidant activity and cold tolerance in native red spruce (*Picea rubens*). Tree Physiol 28:855–862. https://doi.org/10.1093/treephys/28.6.855

Hamburg SP, Yanai RD, Arthur MA, Blum JD, Siccama G (2003) Biotic control of calcium cycling in northern hardwood forests: acid rain and aging forests. Ecosystems 6:399–406

Hornburg V, Lüer B (1999) Vergleich zwischen total- und königswasserextrahierbaren Elementgehalten in natürlichen Böden und Sedimenten. Z Pflanzenernähr Bodenk 162:131–137. https://doi.org/10.1002/(SICI)1522-2624(199903)162:2%3c131:AID-JPLN131%3e3.0.CO;2-1

Huber C, Baier R, Göttlein A, Weis W (2006) Changes in soil, seepage water and needle chemistry between 1984 and 2004 after liming an N-saturated Norway spruce stand at the Höglwald, Germany. Forest Ecol Manag 233:11–20. https://doi.org/10.1016/j.foreco.2006.05.058

IUSS Working Group WRB (2014) World reference base for soil resources 2014. International soil classification system for naming soils and creating legends for soil maps, World Soil Resources Reports No. 106. IUSS Working Group WRB, Rome

Kalinichev AG, Kirkpatrick RJ (2007) Molecular dynamics simulation of cationic complexation with natural organic matter. Eur J Soil Sci 58:909–917. https://doi.org/10.1111/j.1365-2389.2007.00929.x

Kelly SD, Hesterberg D, Ravel B (2008) Analysis of soils and minerals using X-ray absorption spectroscopy. In: Ulery AL, Drees LR (eds) Soil analysis part 5—mineralogical methods. Soil Science Society of USA, Madison, WI, pp 387–464

Kirchner JW, Lydersen E (1995) Base cation depletion and potential long-term acidification of Norwegian catchments. Environ Sci Technol 29:1953–1960. https://doi.org/10.1021/es00008a012

Klysubun W, Sombunchoo P, Deenan W, Kongmark C (2012) Performance and status of beamline BL8 at SLRI for X-ray absorption spectroscopy. J Synchrotron Rad 19:930–936. https://doi.org/10.1107/S0909049512040381

Klysubun W, Tarawarakarn P, Thamsanong N et al (2019) Upgrade of SLRI BL8 beamline for XAFS spectroscopy in a photon energy range of 1–13 keV. Radiat Phys Chem. https://doi.org/10.1016/j.radphyschem.2019.02.004

Kohler M, Wilpert KV, Hildebrand EE (2000) The soil skeleton as a source for the short-term supply of "base cations" in forest soils of the Black Forest (Germany). Water Air Soil Pollut 122:37–48. https://doi.org/10.1023/A:1005277909113

Kubiëna WL (1953) The soils of Europe. Thomas Murby, London

Küfmann C (2006) Measurement and climatic control of eolian sedimentation on snow cover surface in the Northern Calcareous Alps (Wetterstein, Karwendel and Berchtesgadener Alps, Germany). Zeitschr Geomorphol 50:245–268. https://doi.org/10.1127/zfg/50/2006/245

Kunhi Mouvenchery YK, Kucerik J, Diehl S, Schaumann G (2012) Cation-mediated cross-linking in natural organic matter: a review. Rev Environ Sci Biotechnol 11:41–54. https://doi.org/10.1007/s11157-011-9258-3

Lapeyrie F (1988) Oxalate synthesis from soil bicarbonate by the mycorrhizal fungus *Paxillus involutus*. Plant Soil 110:3–8. https://doi.org/10.1007/BF02143532

Likens GE, Driscoll CT, Buso DC et al (1998) The biogeochemistry of calcium at Hubbard Brook. Biogeochem 41:89–173. https://doi.org/10.1023/A:1005984620681

Liu J, Liu HJ, Cui MQ et al (2013) Determination of the calcium species in coal chars by Ca K-edge XANES analysis. Chin Phys 37:028003

Marschner H (1995) Mineral nutrition of higher plants. Academic Press, New York

Messini A, Favilli F (1990) Calcium oxalate decomposing microorganisms; a microbial group of the rhizosphere of forest plants. Ann Microb Enzymes 40:93–101

Mikutta R, Mikutta C, Kalbitz K et al (2007) Biodegradation of forest floor organic matter bound to minerals via different binding mechanisms. Geochim Cosmochim Acta 71:2569–2590. https://doi.org/10.1016/j.gca.2007.03.002

Neuville DR, Cormier L, Flank AM, Briois V, Massiot D (2004) Al speciation and Ca environment in calcium aluminosilicate glasses and crystals by Al and Ca K-edge X-ray absorption spectroscopy. Chem Geol 213:153–163. https://doi.org/10.1016/j.chemgeo.2004.08.039

Paradelo R, Virto I, Chenu C (2015) Net effect of liming on soil organic carbon stocks: a review. Agric Ecosyst Environ 202:98–107. https://doi.org/10.1016/j.agee.2015.01.005

Parfitt RL, Farmer VC, Russell JD (1977a) Adsorption on hydrous oxides I. Oxalate and benzoate on goethite. J Soil Sci 28:29–39. https://doi.org/10.1111/j.1365-2389.1977.tb02293.x

Parfitt RL, Fraser AR, Russell JD, Farmer VC (1977b) Adsorption on hydrous oxides: II. Oxalate, benzoate and phosphate on gibbsite. J Soil Sci 28:40–47. https://doi.org/10.1111/j.1365-2389.1977.tb02294.x

Poszwa A, Dambrine E, Pollier B, Atteia O (2000) A comparison between Ca and Sr cycling in forest ecosystems. Plant Soil 225:299–310. https://doi.org/10.1023/A:1026570812307

Prietzel J, Christophel D (2014) Organic carbon stocks in forest soils of the German Alps. Geoderma 221–222:28–39. https://doi.org/10.1016/j.geoderma.2014.01.021

Prietzel J, Botzaki A, Tyufekchieva N, Brettholle M, Thieme J, Klysubun W (2011) Sulfur speciation in soil by S K-edge XANES spectroscopy: comparison of spectral deconvolution and linear combination fitting. Environ Sci Technol 45:2878–2886. https://doi.org/10.1021/es102180a

Prietzel J, Dechamps N, Spielvogel S (2013) Analysis of non-cellulosic polysaccharides helps to reveal the history of thick organic surface layers on calcareous Alpine soils. Plant Soil 365:93–114. https://doi.org/10.1007/s11104-012-1340-2

Prietzel J, Christophel D, Traub C, Kolb E, Schubert A (2015) Regional and site related patterns of soil nitrogen, phosphorus, and potassium stocks and Norway spruce nutrition in mountain forests of the Bavarian Alps. Plant Soil 386:151–169. https://doi.org/10.1007/s11104-014-2248-9

Prietzel J, Tyufekchieva N, Eusterhues K, Kögel-Knabner I, Thieme J, Paterson D, McNulty I, de Jonge M, Eichert D, Salomé M (2009) Anoxic versus oxic sample pretreatment: effects on the speciation of sulfur and iron in well-aerated and wetland soils as assessed by X-ray absorption near-edge spectroscopy (XANES). Geoderma 153:318–330. https://doi.org/10.1016/j.geoderma.2009.08.015

Prietzel J, Harrington G, Häusler W et al (2016b) Reference spectra of important organic and inorganic phosphate binding forms for soil P speciation using synchrotron-based K-edge XANES spectroscopy. J Synchrotron Rad 23:532–544. https://doi.org/10.1107/S1600577515023085

Prietzel J, Hiesch S, Harrington G, Müller S (2020b) Microstructural and biochemical diversity of forest soil organic surface layers revealed by density fractionation. Geoderma. https://doi.org/10.1016/j.geoderma.2020.114262

Prietzel J, Falk W, Reger B, Uhl E, Pretzsch H, Zimmermann L (2020a) Half a century of Scots pine forest ecosystem monitoring reveals long-term effects of atmospheric deposition and climate change. Glob Change Biol. https://doi.org/10.1111/gcb.15265

Prietzel J, Klysubun W, Werner F (2016a) Speciation of phosphorus in temperate zone forest soils as assessed by combined wet-chemical fractionation and XANES spectroscopy. J Plant Nutr Soil Sci 179:168–185. https://doi.org/10.1002/jpln.201500472

Proffit DL, Fister TT, Kim S et al (2016) Utilization of Ca K-Edge X-ray absorption near edge structure to identify intercalation in potential multivalent battery materials. J Electrochem Soc 163:A2508–A2514. https://doi.org/10.1149/2.0121613jes

Rajendran J, Gialanella S, Aswath PB (2013) XANES analysis of dried and calcined bones. Mat Sci Engin C 33:3968–3979. https://doi.org/10.1016/j.msec.2013.05.038

Rasmussen C, Heckman K, Wieder WR et al (2018) Beyond clay: towards an improved set of variables for predicting soil organic matter content. Biogeochem 137:297–306. https://doi.org/10.1007/s10533-018-0424-3

Ravel B, Newville M (2005) ATHENA, ARTEMIS, HEPHAESTUS: data analysis for X-ray absorption spectroscopy using IFEFFIT. J Synchrotron Rad 12:537–541. https://doi.org/10.1107/S0909049505012719

Rowley MC, Grand S, Adatte T, Verrecchia EP (2020) A cascading influence of calcium carbonate on the biogeochemistry and pedogenic trajectories of subalpine soils, Switzerland. Geoderma 361:114065. https://doi.org/10.1016/j.geoderma.2019.114065

Rowley MC, Grand S, Verrecchia EP (2018) Calcium-mediated stabilisation of soil organic carbon. Biogeochem 137:27–49. https://doi.org/10.1007/s10533-017-0410-1

Sarret G, Isaure MP, Marcus MA et al (2007) Chemical forms of calcium in Ca, Zn- and Ca, Cd-containing grains excreted by tobacco trichomes. Can J Chem 85:738–746. https://doi.org/10.1139/v07-076

Schwartz V, Kölbel M (1992) Vergleich verschiedener Aufschlußmethoden zur quantitativen Erfassung der Elementgesamtgehalte in Abhängigkeit von der Bodenausbildung. Z Pflanzenernähr Bodenkd 155:281–284. https://doi.org/10.1002/jpln.19921550407

Sollins P, Kramer MG, Swanston C et al (2009) Sequential density fractionation across soils of contrasting mineralogy: evidence for both microbial- and mineral-controlled soil organic matter stabilization. Biogeochemistry 96:209–231. https://doi.org/10.1007/s10533-009-9359-z

Sowers TD, Adhikari D, Wang J, Yang Y, Sparks DL (2018a) Spatial associations and chemical composition of organic carbon sequestered in Fe, Ca, and organic carbon ternary systems. Environ Sci Technol 52:6936–6944. https://doi.org/10.1021/acs.est.8b01158

Sowers TD, Stuckey JW, Sparks DL (2018b) The synergistic effect of calcium on organic carbon sequestration to ferrihydrite. Geochem Transact 19:4. https://doi.org/10.1186/s12932-018-0049-4

Stahr K, Böcker R (2014) Landschaften und Standorte Baden-Württembergs. Exkursionsführer. Hohenheimer Bodenkundl Hefte, Hohenheim, p 111

Stevenson F (1994) Humus chemistry—genesis, composition, reactions. Wiley, New York

Ström L, Owen AG, Godbold DL, Jones DL (2005) Organic acid behaviour in a calcareous soil: implications for rhizosphere nutrient cycling. Soil Biol Biochem 37:2046–2054. https://doi.org/10.1016/j.soilbio.2005.03.009

Suess E (1970) Interaction of organic compounds with calcium carbonate. I. Association phenomena and geochemical implications. Geochim Cosmochim Acta 34:157–168. https://doi.org/10.1016/0016-7037(70)90003-7

Sun Q, Li J, Finlay RD, Lian B (2019) Oxalotrophic bacterial assemblages in the ectomycorrhizosphere of forest trees and their effects on oxalate degradation and carbon fixation potential. Chem Geol 514:54–64. https://doi.org/10.1016/j.chemgeo.2019.03.023

Suzuki S (2002) Black tea adsorption on calcium carbonate: a new application to chalk powder for brown powder materials. Colloids Surf A 202:81–91. https://doi.org/10.1016/S0927-7757(01)01063-9

Takahashi Y, Miyoshi T, Yabuki S, Inada Y, Shimizu H (2008) Observation of transformation of calcite to gypsum in mineral aerosols by Ca K-edge X-ray absorption near-edge structure (XANES). Atmos Environ 42:6535–6541. https://doi.org/10.1016/j.atmosenv.2008.04.012

Thyrel M, Backman R, Thånell K et al (2015) Nanomapping and speciation of C and Ca in thermally treated lignocellulosic cell walls using scanning transmission X-ray microscopy and K-edge XANES. Fuel 167:149–157. https://doi.org/10.1016/j.fuel.2015.11.037

Tuason MMS, Arocena JM (2009) Calcium oxalate biomineralization by *Piloderma fallaxin* response to various levels of calcium and phosphorus. Appl Environ Microbiol 75:7079–7085. https://doi.org/10.1128/AEM.00325-09

Verrecchia EP (1990) Litho-diagenetic implications of the calcium oxalate-carbonate biogeochemical cycle in semiarid Calcretes, Nazareth, Israel. Geomicrobiol J 8:87–99. https://doi.org/10.1080/01490459009377882

Verrecchia EP, Braissant O, Cailleau G (2006) The oxalate–carbonate pathway in soil carbon storage: the role of fungi and oxalotrophic bacteria. Cambridge University Press, Cambridge

Vesterdal L, Schmidt IK, Callesen I, Nilsson LO, Gundersen P (2008) Carbon and nitrogen in forest floor and mineral soil under six common European tree species. Forest Ecol Manage 255:35–48. https://doi.org/10.1016/j.foreco.2007.08.015

Wallander H (2000) Uptake of P from apatite by *Pinus sylvestris* seedlings colonised by different ectomycorrhizal fungi. Plant Soil 218:249–256. https://doi.org/10.1023/A:1014936217105

Wang L, Amelung W, Prietzel J, Willbold S (2019) Transformation of organic phosphorus compounds during 1500 years of organic soil formation in Bavarian Alpine forests—a $^{31}$P-NMR study. Geoderma 340:192–205. https://doi.org/10.1016/j.geoderma.2019.01.029

Werner F, Prietzel J (2015) Standard protocol and quality assessment of soil phosphorus speciation by P K-edge XANES spectroscopy. Environ Sci Technol 49:10521–10528. https://doi.org/10.1021/acs.est.5b03096

Weyers E, Strawn DG, Peak D, Moore AD, Baker LL, Cade-Menun B (2016) Phosphorus speciation in calcareous soils following annual dairy manure amendments. Soil Sci Soc Am J 80:1531–1542. https://doi.org/10.2136/sssaj2016.09.0280

Whittinghill KA, Hobbie SE (2012) Effects of pH and calcium on soil organic matter dynamics in Alaskan tundra. Biogeochemistry 111:569–581. https://doi.org/10.1007/s10533-011-9688-6

Wilke BM, Mishra VK, Rehfuess KE (1984) Clay mineralogy of a soil sequence in slope deposits derived from Hauptdolomit (dolomite) in the Bavarian Alps. Geoderma 32:103–116. https://doi.org/10.1016/0016-7061(84)90066-1

Wuddivira MN, Camps-Roach G (2007) Effects of organic matter and calcium on soil structural stability. Eur J Soil Sci 58:722–727. https://doi.org/10.1111/j.1365-2389.2006.00861.x

Yanai RD, Blum JD, Hamburg SP, Arthur MA, Nezat CA, Siccama TG (2005) New insights into calcium depletion in Northeastern Forests. J For 103(14):20. https://doi.org/10.1093/jof/103.1.14